ARTICLE

Otud7a Knockout Mice Recapitulate Many Neurological Features of 15q13.3 Microdeletion Syndrome

Jiani Yin,[1,2] Wu Chen,[3,4,10] Eugene S. Chao,[3,4,10] Sirena Soriano,[1,2,10] Li Wang,[1,2,10] Wei Wang,[1,2] Steven E. Cummock,[2] Huifang Tao,[1,2] Kaifang Pang,[2,6] Zhandong Liu,[2,6] Fred A. Pereira,[8,9] Rodney C. Samaco,[1,2,5] Huda Y. Zoghbi,[1,2,7] Mingshan Xue,[1,3,4] and Christian P. Schaaf[1,2,*]

15q13.3 microdeletion syndrome is characterized by a wide spectrum of neurodevelopmental disorders, including developmental delay, intellectual disability, epilepsy, language impairment, abnormal behaviors, neuropsychiatric disorders, and hypotonia. This syndrome is caused by a deletion on chromosome 15q, which typically encompasses six genes. Here, through studies on OTU deubiquitinase 7A (Otud7a) knockout mice, we identify OTUD7A as a critical gene responsible for many of the cardinal phenotypes associated with 15q13.3 microdeletion syndrome. Otud7a-null mice show reduced body weight, developmental delay, abnormal electroencephalography patterns and seizures, reduced ultrasonic vocalizations, decreased grip strength, impaired motor learning/motor coordination, and reduced acoustic startle. We show that OTUD7A localizes to dendritic spines and that Otud7a-null mice have decreased dendritic spine density compared to their wild-type littermates. Furthermore, frequency of miniature excitatory postsynaptic currents (mEPSCs) is reduced in the frontal cortex of Otud7a-null mice, suggesting a role of Otud7a in regulation of dendritic spine density and glutamatergic synaptic transmission. Taken together, our results suggest decreased OTUD7A dosage as a major contributor to the neurodevelopmental phenotypes associated with 15q13.3 microdeletion syndrome, through the misregulation of dendritic spine density and activity.

Introduction

The proximal part of chromosome 15 long (q) arm is one of the most unstable regions of the human genome, largely due to six low copy repeat (LCR) elements, which are likely to mediate non-allelic homologous recombination (NAHR). These LCR elements often become breakpoints in chromosomal rearrangements and are named breakpoints BP1–BP6.

Chromosomal deletions and duplications are frequently associated with disease. 15q13.3 microdeletions were first described in 2008 as a rare condition associated with intellectual disability and seizures.[1] Current estimate of the frequency of 15q13.3 microdeletion in the general population is 1 in 30,000 to 40,000 individuals, with some sources reporting an even higher frequency.[1–4] Further assessment of clinical implications of 15q13.3 microdeletion suggests that some individuals who carry the deletion may be unaffected, whereas others manifest a wide spectrum of neuropsychiatric symptoms.[2,5,6] Statistically, 55%–75% of affected individuals show developmental delay or cognitive deficits. Seizures or EEG abnormalities have been reported in about one third of individuals (28%–42%). Language impairment and dysmorphic features are often seen (16%–30%). About 10% of individuals meet formal criteria for autism spectrum disorder (MIM: 209850). Finally, a subset of individuals have attention deficit hyperactivity disorder (ADHD), mood disorders, aggression, schizophrenia, and/or hypotonia.[7] Please refer to Lowther et al. for a schematic view of heterozygous and homozygous 15q13.3 microdeletions and a review of the human case subjects.[6]

The 15q13.3 microdeletions commonly encompass six protein-coding genes: FAN1 (MIM: 614817), MTMR10, TRPM1 (MIM: 603576), KLF13 (MIM: 605328), OTUD7A (MIM: 612024), and CHRNA7 (MIM: 118511). Smaller deletions that involve only one exon of OTUD7A and the entire CHRNA7 have been found in individuals who manifest phenotypes similar to affected individuals with larger deletions.[5,8] CHRNA7, which encodes for a nicotinic receptor, has been considered as the major candidate gene to account for the neurological phenotypes of 15q13.3 microdeletion syndrome (MIM: 612001). However, our recent work showed that mice deficient in Chrna7 do not recapitulate the cognitive, behavioral, or electrophysiological phenotypes seen in human individuals,[9] which raises the possibility that OTUD7A may account for the phenotypes associated with 15q13.3 microdeletion syndrome.

[1]Department of Molecular and Human Genetics, Baylor College of Medicine, Houston, TX, USA; [2]Jan and Dan Duncan Neurological Research Institute, Texas Children's Hospital, Houston, TX, USA; [3]Department of Neuroscience, Baylor College of Medicine, Houston, TX, USA; [4]The Cain Foundation Laboratories, Jan and Dan Duncan Neurological Research Institute, Texas Children's Hospital, Houston, TX, USA; [5]Program in Translational Biology and Molecular Medicine, Baylor College of Medicine, Houston, TX, USA; [6]Department of Pediatrics, Baylor College of Medicine, Houston, TX, USA; [7]Howard Hughes Medical Institute, Baylor College of Medicine, Houston, TX, USA; [8]Huffington Center on Aging and Department of Molecular and Cellular Biology, Baylor College of Medicine, Houston, TX 77030, USA; [9]Bobby R. Alford Department of Otolaryngology-Head and Neck Surgery, Baylor College of Medicine, Houston, TX 77030, USA
[10]These authors contributed equally to this work
*Correspondence: schaaf@bcm.edu
https://doi.org/10.1016/j.ajhg.2018.01.005.

Material and Methods

sgRNA and Cas9 Preparation

Donor DNAs expressing sgRNAs under the T7 promoter were prepared by PCR, using Phusion High-Fidelity polymerase (New England Biolabs), pX330 as a template, and a combination of reverse primer with one of two forward primers: forward primer for exon 4 of *OTUD7A* 5′-TTAATACGACTCACTATAGGCTAGC GAGGCGGCATGTAAGGTTTTAGAGCTAGAAATAGC-3′, forward primer for exon 6 of *OTUD7A* 5′-TTAATACGACTCACTATAGG GAAGTGTGTGCGAGGCTCGCGTTTTAGAGCTAGAAATAGC-3′, reverse primer 5′-AAAAGCACCGACTCGGTGCC-3′.

The resulting PCR products were subjected to RNA transcription, using the MEGAshortscript T7 Transcription kit (Thermo Fisher Scientific) with manufacturer's protocol. The sgRNAs were purified by the MEGAshortscript Transcription Clean-Up kit (Thermo Fisher Scientific).

Cas9 was ordered from PNA TECHNOLOGY and stored at −80°C. On the day of microinjection, final concentrations of 30 ng/μL Cas9 and 20 ng/μL sgRNA (total) were mixed into a 150 μL injection buffer (10 mM Tris [pH 7.5], 0.25 mM EDTA) and heated at 37°C for 5 min. After centrifuging at 20,000 × *g* for 10 min at 4°C, the top 2/3 of supernatant was used for cytoplasmic microinjection.

Cytoplasmic Microinjection

C57BL/6J female mice were superovulated and mated with C57BL/6J males, and fertilized eggs were collected from the oviduct. The pronuclear-stage eggs were injected with Cas9 and sgRNAs at the indicated concentrations. The eggs were cultivated in kSOM overnight and then transferred into the oviducts of pseudopregnant FVB females.

Genotyping

The last 1–2 mm of mouse tails were cut into a 1.5 mL Eppendoff tube containing 135 μL 50 mM NaOH and incubated overnight on a 55°C shaker. DNAs were extracted by adding 15 μL Tris-HCL at pH 6.8, and centrifuging at 20,000 × *g* for 1 min.

1 μL of DNA was used for each PCR reaction using Econo taq DNA polymerase (Lucigen, WI). Forward primer for wild-type 5′-TCATGAACCAGCTTCCCTTT-3′, reverse primer for wild-type 5′-GCTAGCATGCAGGGTCACTT-3′, forward primer for mutant 5′-TGTGCACGAGCTGTAAAAGG-3′, reverse primer for mutant 5′-GTGGCAACAACCACTGTCAC-3′. To genotype off-target candidates, primers in Table S1 were used.

Plasmid Preparation

To construct pCMV-3xFLAG-OTUD7A plasmid, human OTUD7A coding regions were PCR amplified and placed into the pCMV10-3xFLAG plasmid between multicloning sites HindIII and XbaI. To construct a pCMV6-OTUD7A-MYC-FLAG, human OTUD7A coding regions together with MYC were PCR amplified from a Myc-DDK-tagged OTUD7A plasmid (Origene Ca. #RC213015) and placed into a pCMV6-FLAG plasmid.

Animals

Mice were maintained on a 14 hr light/10 hr dark cycle, with access to regular mouse chow and water *ad libitum.* For behavioral assessments, heterozygous founders from CRISPR/Cas9 microinjection were backcrossed to wild-type mice (C57BL/6J) for two generations to obtain heterozygous mice for breeding pairs. All of the *Otud7a* homozygous (KO) and heterozygous (HET) mutant mice as well as the wild-type (WT) mice used in our experiments were derived from HET breeding pairs. Mice were randomly assigned and group-housed, with two to five animals per cage, immediately after weaning. Cohort one, consisting of 21 WT, 27 HET, and 15 KO mice, with mixed sex, were monitored for developmental phenotypes. Mice for ultrasonic vocalization recordings (cohort two) consist of 16 WT, 29 HET, and 19 KO mice, with mixed sex. Cohort three, consisting of 14 WT (♂), 20 HET (♂), 14 KO (♂), 14 WT (♀), 20 HET (♀), and 16 KO (♀) mice, went through a series of assays, including elevated plus maze, open field activity, light-dark activity, self-grooming, holeboard exploration, rotarod test, three-chamber test, partition test, forced swimming test, prepulse inhibition, conditioned fear, and nest building, all of which started at 10 weeks of age. Cohort four, consisting of 13 WT (♂), 19 HET (♂), 14 KO (♂), 19 WT (♀), 18 HET (♀), and 13 KO (♀) mice, were monitored for body weight and tested in grip strength and novel object recognition. Experiments were performed during the light cycle, and mice were given inter-test intervals of 1–2 days between each test. All behavioral tests were performed at 700–750 lux illumination and background white noise at approximately 60 dB, with the exception of the partition test, in which there was no background white noise.

For all assays, the experimenter remained blind to the genotypes. All research and animal care procedures were approved by the Baylor College of Medicine Animal Care and Use Committee and were performed in accordance with the relevant guidelines and regulations. The *Otud7a*-null mouse line will be available from The Jackson Laboratory as JAX#031294.

Developmental Assessment

Neurobehavioral development was examined during the pre-weaning period, using a battery of tests that evaluated sensorial and motor responses reflecting the maturation of the CNS, as described previously.[10] The day of appearance of developmental landmarks, including negative geotaxis, cliff aversion, incisor eruption and growth, eye lid opening, and ear opening, was recorded. To evaluate negative geotaxis, pups were placed facedown on a paper box that was tilted 30° from the horizon line. The day when the pup turned around to face upward was recorded. To evaluate cliff aversion, pups were placed with their legs just within the edge of a paper box. The day when the pup avoided falling off the edge was recorded. Incisor growth was evaluated by the appearance of shiny spots at the tip of the incisors.

Ultrasonic Vocalization

Ultrasonic vocalization was recorded on postnatal days 2, 4, 6, 8, and 10. All recordings were performed between 10:00 AM and 4:00 PM. On the first day of recording, the subjects were marked for identification by Sharpie pen on tails or backs, immediately following the recording. On the following days, subjects were re-marked in the same way immediately after recording. On day 10, subjects were ear tagged and the last 1–2 mm of tail was clipped for genotyping. At the time of recording, a litter was separated from its parents and placed in an empty clean cage with beddings heated to 37°C on a heat mat. Temperature at the top of the bedding was monitored with a forehead digital thermometer (BARUN, MA). For each recording, a pup was moved with minimal handling into a cup, which was placed into an anechoic, sound-attenuating chamber (Med Associates Inc.). The pup was then allowed to rest for 1–2 min. Subsequently, audio was recorded

for 2 min using a CM16 microphone (Avisoft Bioacoustics) and amplified/digitized using UltraSoundGate 416H, at a 250 kHz sampling rate and a bit depth of 16, using Avisoft RECORDER software.

Rotarod Test

Motor coordination and motor learning was assessed, using an accelerating rotarod (UGO Basile). Mice at 11 weeks of age were placed on the rotating drum, which accelerated from 4 to 40 rpm over a 5 min period. Time spent walking on top of the rod before falling off was recorded manually, with a maximum time of 5 min. Mice were given four trials per day over 4 consecutive days, with an inter-trial rest interval of more than 30 min.

Prepulse Inhibition

The prepulse inhibition (PPI) was used to evaluate schizophrenia-associated behavior at 13 weeks of age, as described previously.[9] Mice were placed into startle chambers (SR-LAB, San Diego Instruments). The prepulse+pulse trials consisted of a 20 ms prepulse sound, a 100 ms delay, followed by a 40 ms 120 dB startle pulse. Prepulse intensities were 74, 78, and 82 dB. The NOSTIM trial consisted of background noise only. Each trial type was presented six times, in pseudorandom order, with an inter-trial interval of 10 to 20 s. Percent prepulse inhibition of the startle response was calculated for each acoustic prepulse intensity as $100 - [(\text{startle response on the prepulse plus startle stimulus} /\text{startle response alone}) \times 100]$.

Grip Strength

Grip strength was measured at 25 weeks of age. Each mouse was held by the tail and allowed to grasp the middle of the bar of the Chatillon-Ametek grip strength meter (Columbus Instruments) with both of its forepaws. Then the mouse was pulled away from the bar until it released it, and the maximum force generated was recorded. The test was repeated three times for each mouse, and the grip strength values were acquired by averaging the scores from the three pulls.

Behavioral Data Analysis and Statistics

Statistical analysis of genotype and sex effects on behavioral studies were performed using Kruskal-Wallis test, two-, or three-way analysis of variance (ANOVA). If a Kruskal-Wallis test was significant, Dunn's multiple comparison test was performed for between-group comparisons. If an ANOVA was significant, a Tukey's HSD post hoc test or post hoc interaction analysis was performed for between-group comparisons or interaction analysis. Detailed statistical analysis for behavioral data was provided in Table S3. p values of < 0.05 were considered to be statistically significant. All data were presented as mean $\pm$ SEM (GraphPad Prism 6.0e).

Surgery and EEG Recordings

Video EEG and EMGs were acquired from three WT (♂), three KO (♂), three WT (♀), and three KO (♀) animals at 4 months of age. The methods were modified from previous publications.[12] Adult mice at 14 weeks were anesthetized with 1%–2% isoflurane. Under aseptic conditions, each mouse was surgically implanted with the cortical EEG recording electrodes (Teflon-coated silver wire, 127 μm diameter) in the subdural space of the left frontal cortex and the right parietal cortex, respectively, with the reference electrode positioned in the occipital region of the skull.

The third recording electrode (Teflon-coated tungsten wire, 50 μm diameter) was aimed at the dentate gyrus (P2.0R1.8H1.8), with the reference electrode at the corpus callosum. In addition, the fourth recording electrode (silver wire) was inserted into the neck muscles, to monitor the electromyogram (EMG) as an indicator of animal activity level. All electrode wires were attached to a miniature connector (Harwin Connector) and secured on the skull by dental cement. After 2 weeks of post-surgical recovery, simultaneous EEG activity, EMG activity (filtered between 0.1 Hz and 1 kHz, sampled at 2 kHz), and behavior were recorded in freely moving mice for 2 hr per day over a 4 day span.

EEG Data Analysis

EEG data were processed by custom-written algorithms in MATLAB R2015b. Briefly, EEG signals were divided into 10-min segments and each segment was filtered with a third order Butterworth bandpass filter (0.5 and 400 Hz cutoffs). To identify seizure-like events, the filtered data were divided into 500-ms non-overlapping epochs. EEG changes that occurred in the time domain were captured by amplitude correlation (autocorrelation value between successive epochs) and root mean square (average amplitude of the epoch). Changes that occurred in the frequency domain were captured by frequency band ratio, where the power of the upper band (100–300 Hz) was contrasted with that of the lower band (0.5–80 Hz). An EEG segment that exceeded the thresholds for all three of the above quantitative features was identified as a candidate for epileptiform activity. Each candidate and the corresponding video were then visually inspected to confirm as a seizure-like event. For each seizure-like event, the duration (the time difference between the first and last peaks), spike amplitude (the average amplitude of spike peaks), and spike frequency were quantified. To identify repetitive-spike events, the filtered data were divided into 250-ms non-overlapping epochs, and frequency band ratio (0.5–80 Hz for the lower band and 100–300 Hz for the upper band), root mean square, and spike density (number of spikes per epoch) were used. An EEG segment that exceeded the thresholds for all three of the above quantitative features was identified as a candidate and was then visually inspected to confirm as a repetitive-spike event. Data were analyzed blindly to the genotypes.

Primary Neuronal Culture and Transfection

2% B-27 supplement (Life Technology, Ca. 17504-044), 1× GlutaMAX supplement (Life Technology, Ca. 35050-061), and 1× penicillin-streptomycin (Life Technology, Ca. 15140-122), were added to Neurobasal Medium (Thermo Fisher, 21103-049) to make complete Neurobasal Medium for primary cortical neuronal culture. Cortices, together with hippocampi, were dissected out from wild-type and knockout postnatal day 0 pups using sterile dissection tools, and meninges were carefully removed. The last 1–2 mm of their tails were used for genotyping. The cortices from each mouse were placed into 500 μL complete Neurobasal Medium with 10% Fetal Bovine Serum (Thermo Fisher Scientific, Ca. 10439016) in an eppendoff tube, on a 37°C heat block, shaking at 1,000 rpm. After dissection was performed for all mice, tubes were taken out of the shaker to let the tissue settle. Next, supernatants were removed, and tissues were allowed to incubate in 500 μL preheated papain solution from the Papain kit (Worthington Biochemical Corp, Ca. LK003150) on the 37°C shaker for 45 min. Then, supernatants were removed and tissues were triturated rigorously in preheated 500 μL complete

Neurobasal Medium with 1 mL pipette, until no clumps of cell were visible (about 25 times of pipetting up and down). The number of cells was quantified and 1 million cells were plated in complete Neurobasal Medium with 10% Fetal Bovine Serum (FBS) on poly-D-lysine/laminine pre-coated coverslips (Fisher Scientific, Ca. 08-774-385) in 24-well plates. Half of the media was changed with complete Neurobasal medium without FBS on the following day, and then was changed every 3 days until DIV 14 for immunofluorescence.

Primary neurons were transfected with plasmids on DIV 7, using Lipofectamine 2000 (Thermo Fisher, Ca. 11668-019). 300 ng of pEGFP-C1 (Clontech) and 700 ng of pcDNA3 or plasmid that expresses OTUD7A were mixed with 100 μL Neurobasal Medium and 2 μL Lipofectamine 2000, and incubated for 30 min at room temperature. 20 min after incubation, we collected the conditioned media from the primary neuronal cultures and replaced them with 1 mL pre-warmed Neurobasal Medium (without any supplement). When the 30 min incubation time was complete, we added 400 μL of pre-warmed Neurobasal Medium to the 100 μL mixture and changed the media of each well to this 500 μL new mixture. Each well was washed twice with 800 μL Neurobasal Medium after 3–4 hr of incubation at 37°C and was replaced back to the collected conditioned media. Primary neuronal culture and measurement of dendritic spine density have been repeated three times. Spines were quantified from secondary apical dendrites, and the experimenter remained blind to the genotypes. The four spine categories were identified by the same criteria as the following reference.[13]

Immunofluorescence

Immunofluorescence assay was done on DIV 14 in mouse primary neuronal cultures, 24–48 hr after transfection in HeLa cells. Cells were rinsed with 1× PBS once and then fixed with 10% Formalin for 10 min at room temperature. After three cycles of washing with 1× PBS, cells were permeabilized and blocked in 0.1% triton and 2% donkey serum for 30 min. Cells were then incubated with primary antibodies: mouse anti-FLAG (Sigma, Ca. F1804) and chicken anti-GFP (Abcam, ab13970), at 4°C overnight. After three cycles of washing with 1× PBS, cells were incubated with donkey anti-chicken Alexa488 or anti-mouse Cy3 (Thermo Fisher) secondary antibodies at 1:500, for 1 hr at room temperature. After three cycles of washing with 1× PBS, cells were mounted in mounting medium containing DAPI and imaged with a confocal microscope (Zeiss 880) on the following days.

Golgi-Cox Staining

Three WT and three KO female mice at 4 weeks of age were used. Animals were deeply anesthetized and brains were removed. Golgi-Cox staining was performed using an FD Rapid GolgiStain Kit (FD NeuroTechnologies) according to the manufacturer's instructions. The coronal brain blocks were immersed in a solution of equal parts solutions A and B at room temperature for 2 weeks and then soaked in solution C at 4°C for 48 hr. After freezing with isopentane and embedding in OCT medium, the brain samples were sliced into 50 μm pieces at −22°C using a cryostat microtome. Each frozen section was mounted with solution C on a 0.5% gelatin-coated glass slide. Slides were allowed to dry naturally at room temperature and were then stained with a mixture (solution D: solution E: DW; 1:1:2) for 5 min, after which the slides were rinsed in distilled water twice for 4 min each. Slides were dehydrated in an ascending ethanol series and then sealed with cytoseal (Thermo Fisher Scientific) through xylene.

Bright-field images of basal dendrites of pyramidal neurons from frontal association cortex (FrA), motor cortex (M1/M2), and somatosensory cortex (S1/S2) were acquired using a confocal microscope (Zeiss 880) with z stacks. Dendritic spines were manually counted (from 20 WT FrA, 16 WT M1/M2, 19 WT S1/S2, 19 KO FrA, 18 KO M1/M2, 18 KO S1/S2 dendrites) by an experimenter who was blind to the genotypes, and statistical analysis was performed using two-way ANOVA followed by Bonferroni's multiple comparisons test.

Frontal Cortical Slice Electrophysiology

Acute fresh coronal slices (350 μm thick) containing frontal cortex were prepared from 8- to 11-week-old mice with a vibratome slicer (Leica Microsystems). Acute slices were collected in chilled (2°C–5°C) cutting solution containing (in mM) 110 choline-chloride, 25 $NaHCO_3$, 25 D-glucose, 11.6 sodium ascorbate, 7 $MgSO_4$, 3.1 sodium pyruvate, 2.5 KCl, 1.25 NaH_2PO_4, and 0.5 $CaCl_2$. Then, slices were incubated in standard artificial cerebrospinal fluid (ACSF, in mM) containing 119 NaCl, 26.2 $NaHCO_3$, 11 D-glucose, 3 KCl, 2 $CaCl_2$, 1 $MgSO_4$, and 1.25 NaH_2PO_4 at 37°C for 30 min before being stored at room temperature for recording. All solutions were saturated with 95% O_2 and 5% CO_2.

Whole-cell recordings were made from visually identified pyramidal neurons in layer 2/3 regions of frontal cortices by using a patch clamp amplifier (MultiClamp 700 B, Molecular Devices). Microelectrodes with resistance of 2–3 MΩ were pulled from borosilicate glass capillaries (Sutter Instruments). The intrapipette solution for recording mEPSC (holding at −70 mV) contained (in mM) 140 potassium gluconate, 5 KCl, 10 HEPES, 0.2 EGTA, 2 $MgCl_2$, 4 MgATP, 0.3 Na_2GTP, and 10 Na2-phosphocreatine (pH 7.2). Picrotoxin (100 μM), D-2-amino-5-phosphonopentanoic acid (AP5, 50 μM), and Tetrodotoxin (TTX, 0.1 μM) were present in the ACSF for mEPSC recording.

The whole-cell recording was performed at (30°C ± 1°C) by using an automatic temperature controller (Warner Instrument). Data acquisition was performed by using a digitizer (DigiData 1440A, Molecular Devices). Minianalysis 6.0.7 (Synaptosoft Inc) and pClamp 10 (Molecular Devices) were used for data analysis. Data were discarded when the resistance change was greater than 20% during the course of the experiment. Data are shown as mean ± standard error of mean and analyzed by Mann-Whitney test.

Results

Generation of Otud7a Knockout Mice

Given that the smallest deletion found in individuals with 15q13.3 microdeletion syndrome removes CHRNA7 and part of OTUD7A[5] and that OTUD7A is mainly expressed in the central nervous system (GTEx database), we set out to generate a knockout mouse model of Otud7a. We designed two sgRNAs that delete most of the OTU deubiquitinase domain, which created a premature stop codon in exon 8. Using cytoplasmic microinjection of the sgRNAs, along with Cas9 into 1-cell stage C57BL/6J embryos (Figure 1), we obtained deletions at the desired locus and of the expected size. These deletions were validated by tail DNA sequencing of founder mice and their offspring (Figure 1). No off-target mutations were found
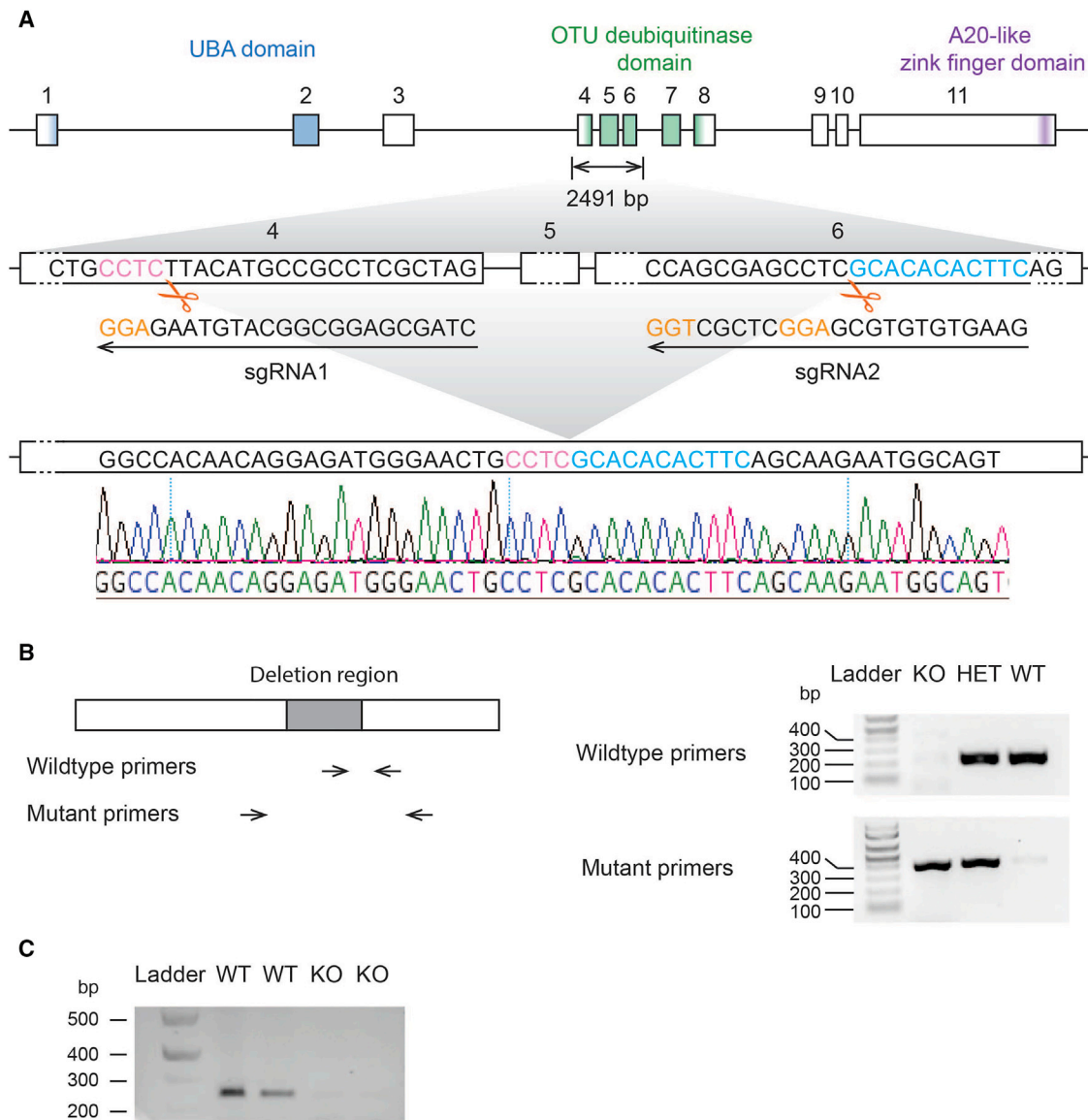
Figure 1. Generation of the *Otud7a* Knockout Mouse Model

(A) Scheme of *Otud7a* knockout design and sequencing validation. Exons of *Otud7a* are boxed, whereas introns are represented by lines in between exons. All exons and introns are plotted in scale within their category. Three domains have been identified in OTUD7A: the UBA domain, OTU deubiquitinase, and an A20-like zinc finger domain. The nucleotides encoding these domains are colored blue, green, and purple, respectively. NGG sequences in the two sgRNAs are shown in orange. Following CRISPR/Cas9 manipulation, we obtained mice with knockout of the expected region, bordering sequences of which are highlighted in pink and blue. Sequencing trace from tail DNA of the mice are shown at the bottom.

(B) Genotype identification of *OTUD7A*-deficient mice. The knockout region was boxed in gray. Genotyping primer binding regions for wild-type and knockout primer sets were indicated by arrows. In the representative genotyping results, animals that carry a wild-type allele show bands at 223 bp with wild-type primers, and those that carry a knockout allele show bands at 389 bp with mutant primers.

(C) RT-PCR products with RNA extracted from brains of wild-type and *Otud7a* knockout mice showing a deficiency of *Otud7a* transcripts in the knockout animals. Primers used for RT-PCR bind to exon 3 and 8 respectively. Forward primer: 5′-GGACTTCAGGAGCTTCATCG-3′, reverse primer: 5′-ACCTCCAAGGGCAGGTAGAT-3′. Expected PCR product size is 244 bp.

by sequencing the top 15 off-target candidates for each sgRNA predicted by CRISPR design tool (Table S1).

Behavioral and Electroencephalographical Abnormalities in *Otud7a* Knockout Mice

In an attempt to address whether *Otud7a* has an effect on phenotypes in close relation to 15q13.3 microdeletion syndrome, we compared *Otud7a* homozygous and heterozygous knockout mice with wild-type littermates, using a battery of 16 behavioral paradigms and electroencephalography (EEG)/electromyography (EMG) recordings (Table 1). Although there was little difference in disease expression between male and female affected individuals, we performed all behavioral and electrophysiological assays on both male and female *Otud7a* knockout mice.

Table 1. Behavioral Assays Used in Correlation to Clinical Manifestations of 15q13.3 Microdeletion Patients

Patient Phenotype	Behavioral Test	Cohort	Age (weeks)
Developmental delay	developmental milestones	1	0–2
Language impairment	ultrasonic vocalization	2	0–1.5
Intellectual disability	conditioned fear	3	13
	novel object recognition	4	27
Motor deficits	rotarod	3	11
Schizophrenia	prepulse inhibition	3	13
Autism (social interaction deficits)	three-chamber test	3	12
	partition test	3	12
	nest building	3	14
Autism (repetitve behaviors)	self-grooming	3	10
	holeboard exploration	3	10
Hypotonia	grip strength	4	25
Anxiety	elevated plus maze	3	10
	light-dark box exploration	3	10
Hyperactivity	open field activity	3	10
Depression	forced swimming test	3	12

Cohort 1: 21 WT, 27 HET, and 15 KO
Cohort 2: 16 WT, 29 HET, and 19 KO
Cohort 3: 14 WT (♂), 20 HET (♂), 14 KO (♂), 14 WT (♀), 20 HET (♀), and 16 KO (♀)
Cohort 4: 15 WT (♂), 18 HET (♂), 19 KO (♂), 18 WT (♀), 15 HET (♀), and 16 KO (♀)

Developmental delay and intellectual disability are the most prevalent phenotypes (50%–60%) seen in individuals with 15q13.3 microdeletions.[7] We therefore assessed development in our *Otud7a* mutant mouse model. We found that *Otud7a* homozygous null mice presented a significant preweaning growth delay, as they had a 30% weight reduction compared to heterozygous knockout or wild-type littermates (Figure 2A). This finding is in accordance with the fact that five out of seven individuals with 15q13.3 homozygous microdeletions reported growth rates below 3rd percentile at 9–10 years of age.[3,4,14–16] The overall brain structure and organization in homozygous null mice appears normal (data not shown). To further evaluate the neurobehavioral development of *Otud7a* mice, we monitored pups of different genotypes every day, from postnatal day 0 to 14, and recorded the day on which they reached various developmental milestones. These milestones included negative geotaxis, cliff aversion, incisor eruption/growth, eye lid opening, and ear opening. We found that *Otud7a*-null mice had significant delay in almost all the milestones measured, with the exception of eye lid and ear opening

(Figure 2B). However, there were no memory and learning deficits in adult *Otud7a*-null mice, as measured by fear conditioning and novel object recognition tests (Figures S1A–S1C).

All 15q13.3 homozygous microdeletion individuals and about 40% of heterozygous individuals have either a history of seizures or abnormal electrographic changes.[7] To evaluate the impact of *Otud7a* on brain activity, we recorded video-electroencephalography (EEG) and electromyography (EMG) in freely moving mice. We observed abnormal repetitive-spike events in all of the three male and three female *Otud7a*-null mice but not in any of the three male and three female wild-type littermates (Figures 3A and 3B; Table 2). Furthermore, we observed seizure-like events associated with behavioral arrest (see Movie S1 for example) in three out of six *Otud7a*-null mice, but not in any of the wild-types littermates (Figures 3C–3E; Table 2). Interestingly, instead of a generalized excessive or synchronous electrical discharge in the entire brain, these epileptiform activities were more prominent in the frontal cortex than the parietal cortex (Figures 3C–3E).

Language disability has been reported in all 15q13.3 homozygous microdeletion individuals and about 30% of heterozygous individuals.[7] In equivalence, we characterized ultrasonic vocalizations in pups of all three genotypes on postnatal day 2, 4, 6, 8, and 10, which was frequently used to assess vocalization and communication in rodents.[17–19] We found that mutant mice had an impairment in an *Otud7a* dosage-dependent manner, which was significant on day 8 (Figure 2C). Given that a subset of 15q13.3 microdeletion individuals have been diagnosed with autism spectrum disorder, which typically features social communication deficits, repetitive behaviors, and restricted interests, we also assessed social interaction and repetitive behaviors in *Otud7a* mice (Table 1). Results from these assays suggest that *Otud7a* deficiency leads to various differences in social behaviors in mice, which may or may not indicate autistic-like behaviors (Figures S1D–S1I).

Because all homozygous 15q13.3 microdeletion individuals reported in the literature had hypotonia and were nonambulatory, we tested *Otud7a* mice for open field activity, grip strength, and performance on a rotating rod. We found that *Otud7a*-null mice were not significantly different from wild-type littermates in the distance traveled in the open field assay (Figure S1M). However, *Otud7a*-null mice had significantly reduced grip strength compared to their wild-type littermates (Figure 2D). Furthermore, *Otud7a*-null mice showed significant impairment in rotarod performance (Figures 2E and 2F), which suggests a deficit in motor coordination and motor learning.

Other neuropsychiatric and behavioral phenotypes, including attention deficit and hyperactivity disorder (ADHD), anxiety, and depression, have occasionally been reported in 15q13.3 microdeletion individuals. *Otud7a*-null mice did not show any significant differences from their wild-type littermates in any of the relevant assays that test for these conditions (Figures S1J–S1N). However,
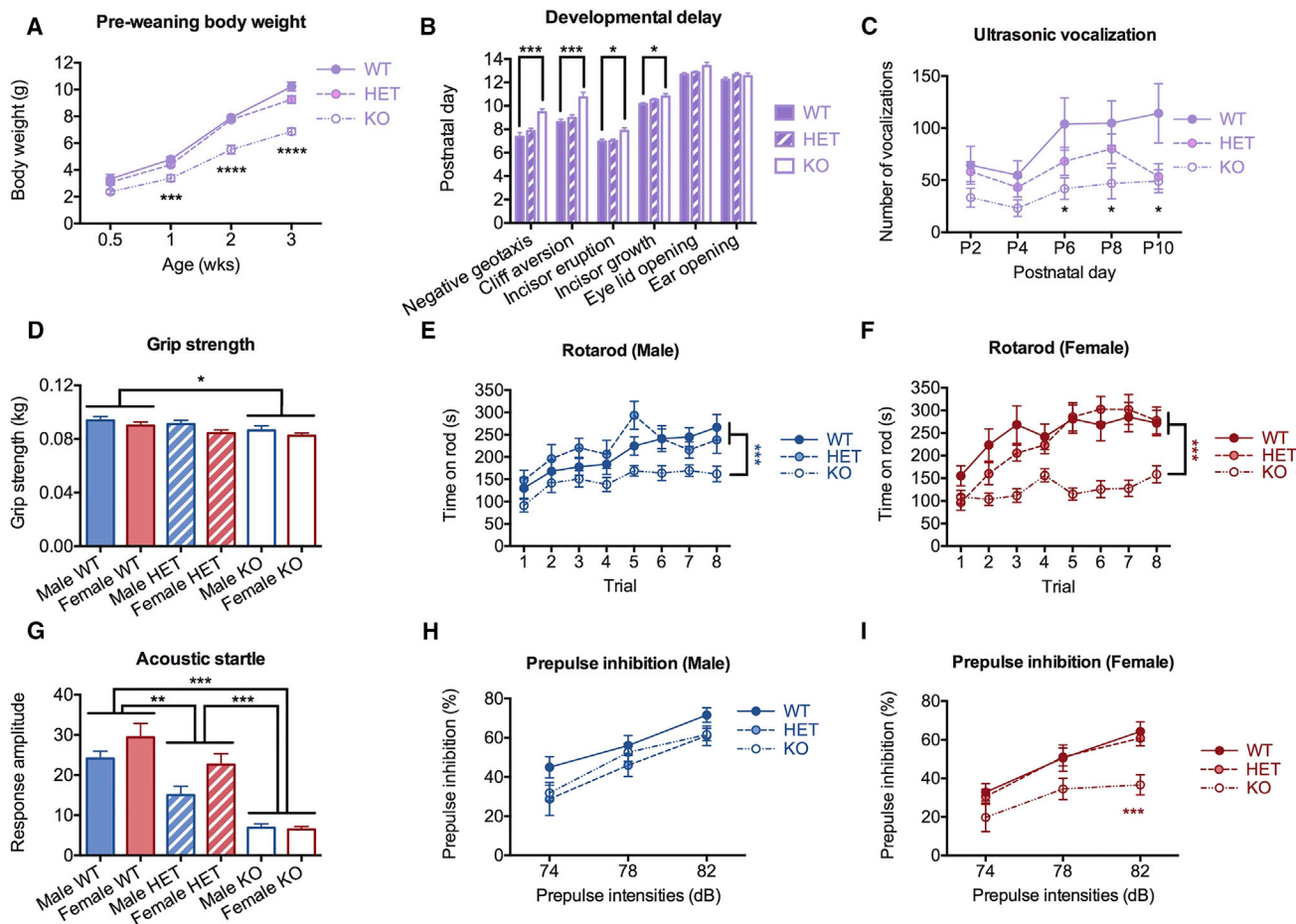
Figure 2. Mice Deficient in *Otud7a* Show Cardinal Phenotypes Related to 15q13.3 Microdeletion Syndrome

Data from male and female mice were combined for behavioral tests performed during pre-weaning period and were shown as bars or lines in purple. Behavioral data from male and female adult mice were shown separately, with males in blue and females in red.

(A) Null mice have decreased body weight prior to weaning.

(B) Null mice show developmental delay.

(C) Null mice show impaired ultrasonic vocalization.

(D) Null mice have reduced grip strength.

(E and F) Both male and female null mice show impairment in rotarod performance.

(G) Homozygous and heterozygous *Otud7a* knockout mice show reduced acoustic startle response.

(H and I) Male (H) and female (I) null mice manifest deficits in prepulse inhibition.

Data are presented as mean $\pm$ SEM (*p < 0.05, **p < 0.01, ***p < 0.001, ****p < 0.0001).

when we measured sensorimotor gating, a feature impaired in schizophrenia that has also been reported in 15q13.3 microdeletion individuals, we found that both homozygous and heterozygous *Otud7a* knockout mice had impaired acoustic startle response (Figure 2G). Additionally, female *Otud7a* homozygous null mice showed reduced prepulse inhibition at 82 dB prepulse intensity (Figure 2H). We tested hearing abilities of male and female *Otud7a* mutant mice using auditory brainstem response (ABR) and distortion product otoacoustic emissions (DPOAE) tests. We found that *Otud7a* mutant mice had no significant hearing loss at the age when they were tested for prepulse inhibition (Figure S2). These data suggest that female *Otud7a*-null mice have sensory-gating deficits.

One of the main questions regarding 15q13.3 microdeletion syndrome relates to the contribution of individual genes within the locus to the overall clinical phenotype. We therefore compared the phenotypes of our *Otud7a*-null mice with the established 15q13 microdeletion mouse model ($Df(h15q13)^{-/-}$), which had a deletion encompassing all six genes[20] (Table 3). The only behavioral abnormality present in the microdeletion mouse model that was not present in *Otud7a*-null mice is a learning and memory deficit. Otherwise, *Otud7a*-null mice recapitulated the cardinal phenotypes of the 15q13 deletion mouse as well as the main clinical aspects of the human microdeletion syndrome.

Role of Otud7a in Regulation of Dendritic Spine Density and Activity

Next, we began to investigate the cellular and molecular functions of *OTUD7A*, which were largely unknown.
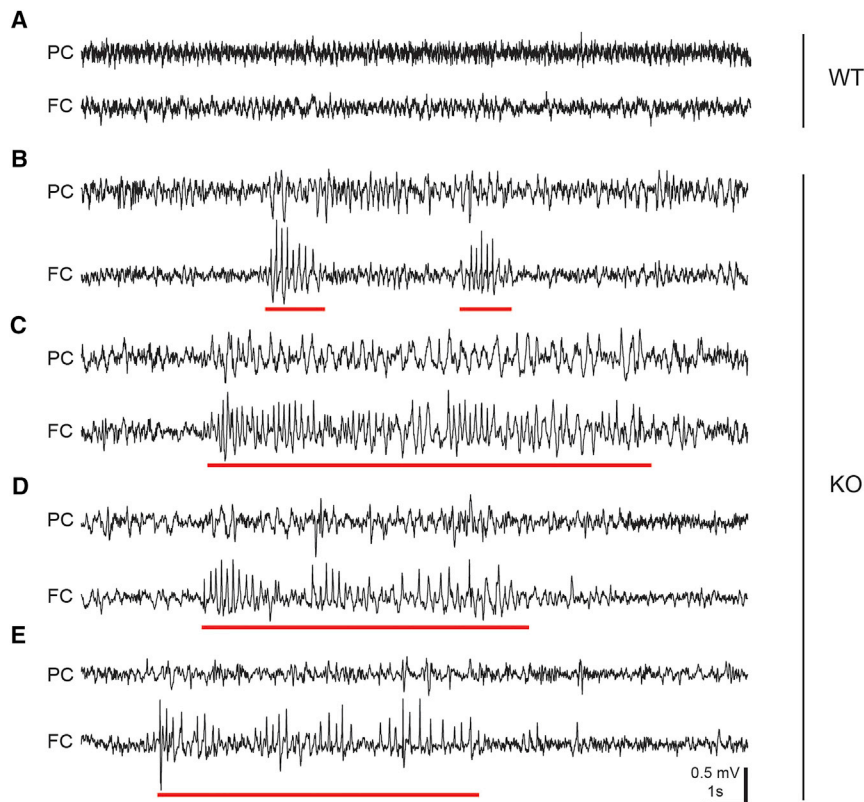
Figure 3. Abnormal EEG and Epileptiform Activities in *Otud7a*-Null Mice

Representative EEG traces from the parietal and frontal cortices of one WT (A) and four different null (B–E) mice. Red lines indicate the abnormal repetitive-spike events (B) or seizure-like events manifesting phenotypically as behavioral arrest (C–E). The seizure-like events lasted for 9.11 ± 0.98 s. The spike amplitude and frequency were 0.42 ± 0.02 mV and 4.77 ± 0.22 Hz, respectively. The data were obtained from 23 events in 3 mice and presented as mean ± SEM. Note, the data were also presented in Table 2 for each mouse. Abbreviations: PC, parietal cortex; FC, frontal cortex.

A published RNA-seq transcriptome database of different cell types in mouse cerebral cortexes showed that *Otud7a* has a relatively higher expression in neurons and oligodendrodyte progenitor cells compared to other cell types in the central nervous system.[21] Due to a lack of Otud7a-specific antibodies, we investigated the localization of N-terminally FLAG-tagged OTUD7A in mouse primary cortical neurons and observed an enrichment of OTUD7A at dendritic spines and membrane compartments in the cell body. Membrane localization of OTUD7A was also observed with a different construct expressing C-terminally Myc-FLAG tagged OTUD7A in HeLa cells (Figure S3), which is in contrast to the reported cytoplasmic localization of its homolog OTUD7B.[22] The reason for the differing localization of the two homologs may be the presence of lipid modification sites in OTUD7A, which are not present in OTUD7B (Table S2).

The distinct localization at dendritic spines suggests a potential role of OTUD7A in the regulation of synaptogenesis and synaptic plasticity. Therefore, we compared the number of spines in primary cortical neurons from *Otud7a*-null mice to those of their wild-type littermates, which revealed a significant reduction in spine density in the null mice (Figure 4B). The reduction of dendritic spine density in primary neurons from null mice was rescued by overexpressing OTUD7A (Figure 4B), which supports the notion that the phenotypes in *Otud7a* knockout mice were due to loss of OTUD7A function rather than a potential dominant-negative effect.

Enlightened by a companion manuscript in this issue of *AJHG* that utilizes a complementary approach to study *OTUD7A*,[23] we also examined its role in dendritic morphology of primary neurons. No significant difference in dendritic complexity was observed using Sholl analysis between primary cortical neurons from *Otud7a*-null mice and their wild-type littermates. However, overexpression of *Otud7a* led to significantly increased dendritic arborizations (Figure S4).

We performed Golgi-Cox staining of various cortical regions from *Otud7a*-null mice and wild-type littermates to investigate whether dendritic spine density was also decreased *in vivo*. We found that *Otud7a*-null mice had a decreased number of dendritic spines in the frontal cortex and motor cortex but not in the somatosensory cortex (Figure 5A), which was in line with observations in 15q13.3 microdeletion mice.[23] To determine whether decreased spine density may lead to an impairment in glutamatergic synaptic transmission, we performed whole-cell recording of miniature excitatory postsynaptic currents (mEPSCs) in frontal cortices of *Otud7a*-null and wild-type littermates. We found a reduction in the frequency of mEPSCs in knockout mice, while the amplitude of mEPSCs was unchanged (Figure 5B). Taken together, the decreased dendritic spine density and the decreased mEPSC frequency indicates that *Otud7a* deficiency reduces the number of functioning excitatory synapses.

Discussion

In summary, our results show that *Otud7a* heterozygous and homozygous knockout mice have recapitulated cardinal phenotypes associated with 15q13.3 microdeletion syndrome. Heterozygous mice show reduced ultrasonic vocalization and acoustic startle deficit, and homozygous knockout mice recapitulate developmental delay, vocal

Table 2. Quantification of Repetitive-Spike Events and Seizure-like Events

Mouse ID	Genotype	Rate of Repetitive-Spike Events (#/hour)	Number of Seizure-like Events	Rate of Seizure-like Events (#/hour)	Duration of Seizure-like Events (s)	Spike Amplitude in Seizure-like Events (mV)	Spike Frequency in Seizure-like Events (Hz)
C371	KO	20.63	4	0.50	7.91 ± 0.22	0.32 ± 0.01	4.79 ± 0.13
C372	KO	5.62	0	0	N/A	N/A	N/A
C374	KO	11.38	0	0	N/A	N/A	N/A
C375	KO	59.37	15	1.88	9.35 ± 1.47	0.47 ± 0.03	4.39 ± 0.22
C399	KO	1.00	0	0	N/A	N/A	N/A
C400	KO	0.83	4	0.67	9.42 ± 1.43	0.35 ± 0.01	6.19 ± 0.50

No repetitive-spike events or seizure-like events was observed in wild-type littermates.

impairment, seizure-related abnormalities, motor deficits, hypotonia, and acoustic startle deficit. It is not uncommon to see that mouse neurobehavioral phenotypes are milder when compared with humans. For several human disorders that are pathogenic in heterozygous state, the mouse model is not or is barely significant in heterozygous state, but is convincingly significant in homozygous state. Examples include *SHANK3* for Phelan-McDermid syndrome,[24] *RAI1* for Smith-Magenis syndrome,[25] and *MECP2* in females for Rett syndrome.[26]

Our results, together with findings from the companion manuscript,[23] suggest that *OTUD7A* deficiency largely accounts for phenotypes associated with 15q13.3 microdeletion syndrome and that *OTUD7A* is important in regulation of dendritic spine density and activity. Our finding that *OTUD7A* is crucial for the development and functioning of central nervous system is also well supported by a pLI (probability of loss-of-function intolerance) score of 0.97 in the ExAC database. In ExAC, loss-of-function variants were found at a rate of 1 in every 10,223 individuals enrolled in their study of presumably unaffected individuals. Detailed neuropsychiatric phenotypic information is not available for those individuals. The development of therapeutic intervention for 15q13.3 microdeletion syndrome should take OTUD7A haploinsufficiency into consideration, and future work should

Table 3. Comparison of Behavioral and Electrophysiological Phenotypes between 15q13.3 Homozygous Knockout Mice and *Otud7a*-Null Mice

Phenotypes/Behavioral Assays	Df(h15q13)−/−	Otud7a−/−
Body weight	decreased	decreased
Ultrasonic vocalization	impaired	impaired
Acoustic startle	impaired	impaired
Prepulse inhibition	impaired	impaired
Grip strength	decreased	decreased in female, trend toward decrease in male
Seizures/EEG recording	altered seizure response to PTZ administration	spontaneous EEG abnormalities
Open field	no significant change	no significant change
Three-chamber test	no impairment	no impairment
Developmental delay	not assessed	developmental delay
Rotarod performance	not assessed	impaired
Elevated plus maze	not assessed	no significant change
Novel object recognition	not assessed	no significant change
Forced swimming	not assessed	no significant change
Partition test	not assessed	no impairment
Morris water maze	inconclusive due to vision impairment	not assessed due to motor deficits
Nest building[a]	impaired	trend toward impairment but no significant change
Fear conditioning	decreased cued fear memory	no significant change in female, increased cued fear memory in male

Reference for behavioral phenotypes in Df(h15q13)−/− mice: Forsingdal et al.[20]
[a]In the Df(h15q13)−/− study, 6 knockout mice with mixed gender were assessed. In our study, 14 male Otud7a−/− mice and 16 female Otud7a−/− mice were assessed.
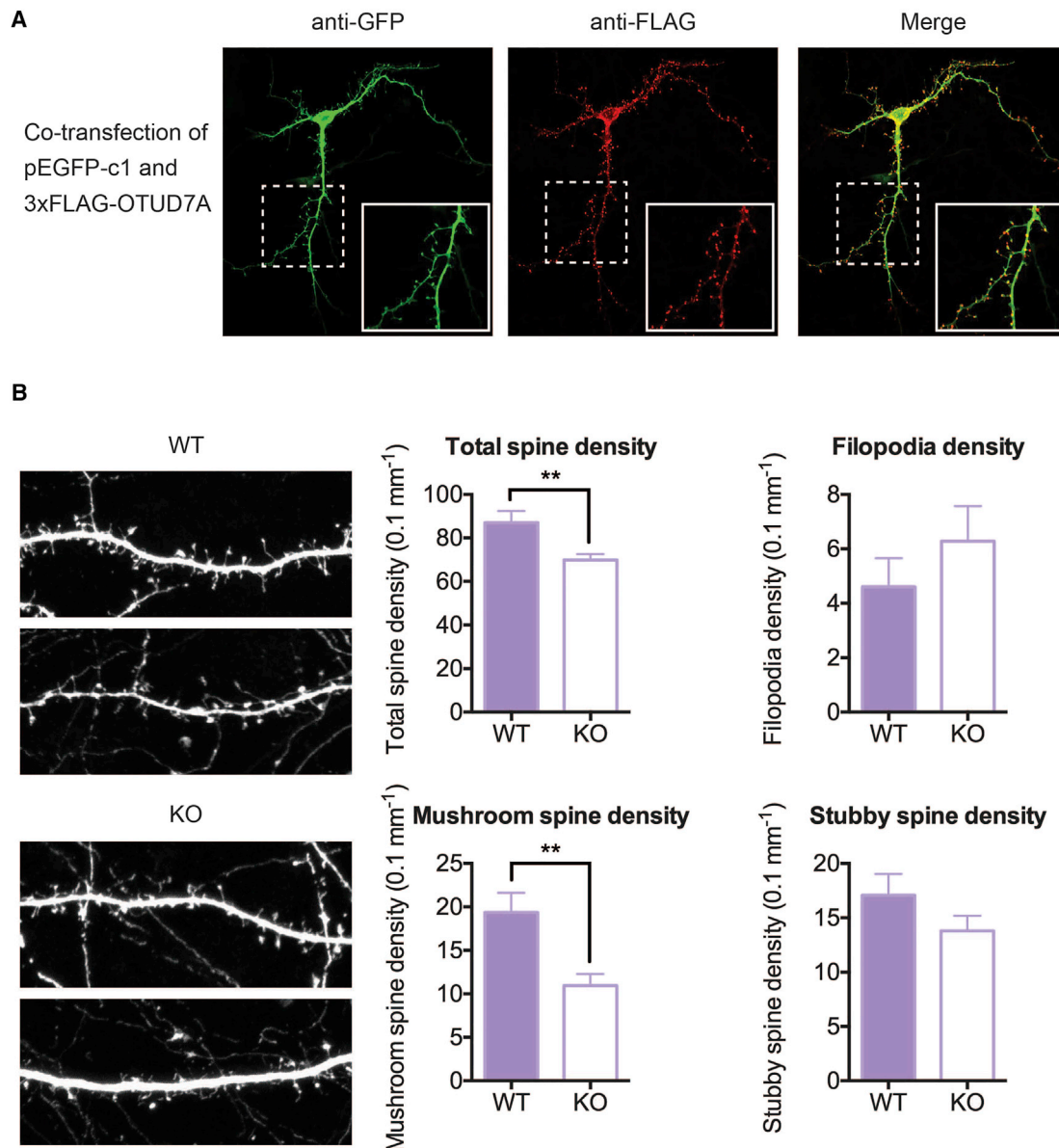
Figure 4. OTUD7A Localizes to Dendritic Spines and Regulates Spine Density

(A) OTUD7A localizes to dendritic spines. Mouse primary cortical cultures were co-transfected with pEGFP-c1 and 3xFLAG-OTUD7A on DIV 7. On DIV 14, immunofluorescent imaging was performed, with GFP in green (Alexa488) and FLAG in red (Cy3). The bottom right corner of each image shows a magnification of the inset box.

(B) Primary cortical neurons from *Otud7a*-null mice show decreased total spine density compared to wild-type neurons, which are rescued by overexpression of *Otud7a*. To compare between genotypes, primary cortical neurons from *Otud7a*-null mice or wild-type littermates were transfected with pEGFP-c1 and stained with GFP antibody. As a rescue experiment, primary neurons from *Otud7a*-null mice were transfected with 700 ng 3xFLAG-OTUD7A per 24-well. We investigated 42 neurons/dendrites from 9 null mice, 41 neurons/dendrites from 3 wild-type mice, and 31 neurons/dendrites from 9 null mice in the rescue experiments. Top: representative examples of dendritic segments of the immune-stained neurons. Bottom: quantification of dendritic spines. Statistical significance was assessed using two-tailed t test. Data are presented as mean ± SEM (*$p < 0.05$, **$p < 0.01$, ***$p < 0.001$).

involve the investigation of molecular pathways regulated by OTUD7A.

Given that cognitive and social deficits were not observed in *Otud7a* knockout mice, genetic background or other genes associated with the deletions may complement and interact with *Otud7a* to contribute to disease manifestation. Future investigations may involve (1) an assessment of the consequences of *Otud7a* loss of function in mice of various genetic backgrounds, (2) rescuing 15q13.3 homozygous knockout mice with transgenes expressing *Chrna7* or *Otud7a*, or (3) the generation of mice with deletion of both *Chrna7* and *Otud7a*.

We observed no dendrite growth defects in *Otud7a* homozygous knockout mice, while 15q13.3 microdeletion mice had decreased cortical neuron dendritic complexity.[23] This indicates that *Otud7a* is not necessary for
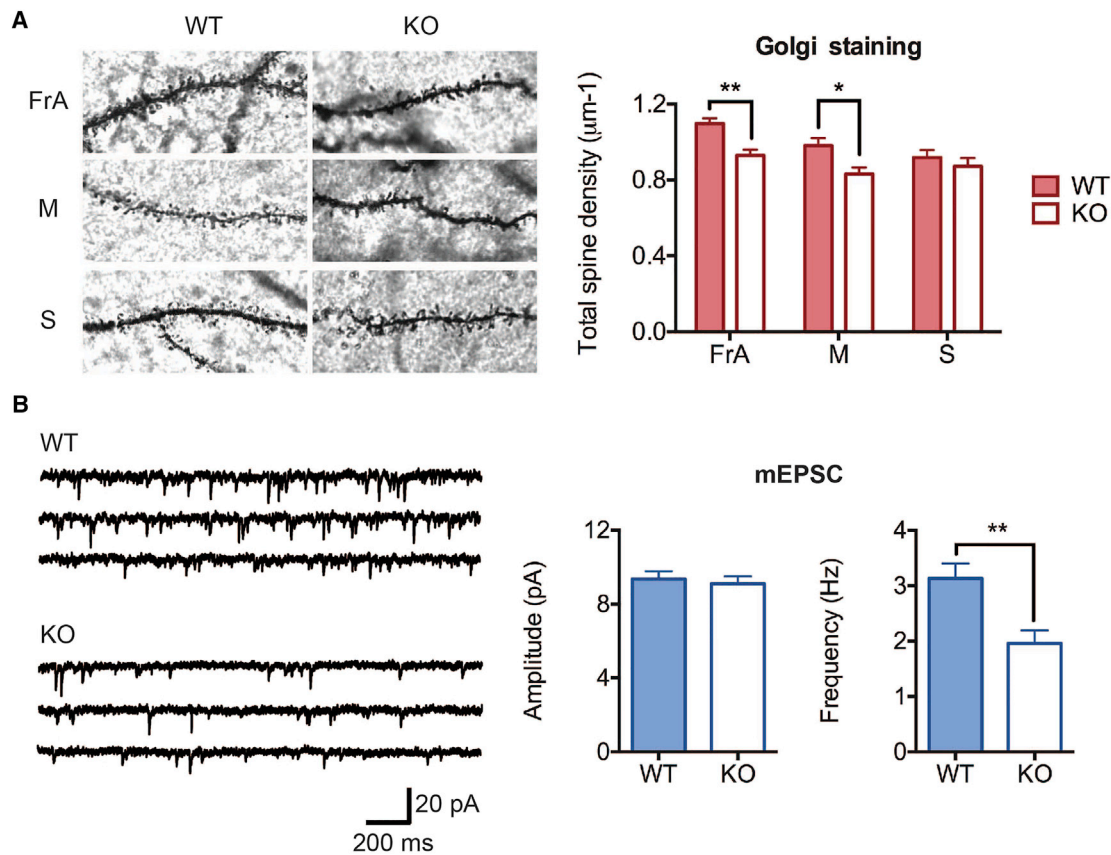
Figure 5. *Otud7a*-Null Mice Display Significantly Reduced Number of Functioning Excitatory Synapses
(A) Golgi-Cox staining shows significantly reduced number of dendritic spines in the frontal association cortex (FrA) and motor cortex (M) but not in the somatosensory cortex (S). Data were obtained from basal dendrites of layer II/III pyramidal neurons (n = 16–20) from 3 null and 3 wild-type female mice at 4 weeks old. Left: representative examples of dendritic segments of the Golgi-Cox stained neurons. Right: quantification of dendritic spine densities.
(B) *Otud7a*-null mice display significantly reduced mEPSC frequency in frontal cortices. Left: sample traces of mEPSCs. Right: average of amplitude and frequency of mEPSCs. Whole-cell recordings were performed on layer II/III pyramidal neurons from four null (n = 11) and four wild-type (n = 15) male mice at 8 to 11 weeks old. Data are presented as mean ± SEM (*p < 0.05, **p < 0.01).

dendritic growth. However, the fact that overexpression of *Otud7a* significantly promoted dendritic arborization and that the dendritic growth defects in neurons from 15q13.3 microdeletion mice were rescued by overexpression of either *Otud7a* or *Chrna7*[23] suggest that *Otud7a* has the capacity to regulate dendritic growth.

Some groups claimed to have identified small deletions in individuals that encompass only *CHRNA7*,[8,16,27] but we found that several of the reported deletions affected also the first exon of *OTUD7A*. In the article by Liao et al.,[3] array CGH identified a deletion that included part of *OTUD7A*, although the undeleted region of *OTUD7A* seemed to be adequate for binding of a bacterial artificial chromosome (BAC) FISH probe. The same is true for the article by Masurel-Paulet et al.:[16] part of *OTUD7A* were involved in the smallest deletions. In the article by Prasun et al.,[28] the lack of coverage at the 5′ region of *OTUD7A* prevented to assess its possible rearrangement. The first exon of *OTUD7A* locates in a segmental duplication and is thus susceptible to chromosome rearrangements. The deletion of the first exon or 5′ region could obviously affect regulation and expression of the respective gene. Analysis

of *OTUD7A* mRNA expression in cell lines generated from the affected individuals with small deletions would be necessary to further investigate the consequences of the respective genomic deletions.

Supplemental Data

Supplemental Data include four figures, three tables, and one movie and can be found with this article online at https://doi.org/10.1016/j.ajhg.2018.01.005.

Acknowledgments

Web Resource

CRISPR design tool, http://crispr.mit.edu/
dbGaP (phs000424.v7.p2), http://www.ncbi.nlm.nih.gov/gap
ExAC Browser, http://exac.broadinstitute.org/gene/ENSG00000169918
GTEx Portal, https://www.gtexportal.org/home/gene/OTUD7A
OMIM, http://www.omim.org/

References

1. Sharp, A.J., Mefford, H.C., Li, K., Baker, C., Skinner, C., Stevenson, R.E., Schroer, R.J., Novara, F., De Gregori, M., Ciccone, R., et al. (2008). A recurrent 15q13.3 microdeletion syndrome associated with mental retardation and seizures. Nat. Genet. *40*, 322–328.

2. van Bon, B.W.M., Mefford, H.C., Menten, B., Koolen, D.A., Sharp, A.J., Nillesen, W.M., Innis, J.W., de Ravel, T.J.L., Mercer, C.L., Fichera, M., et al. (2009). Further delineation of the 15q13 microdeletion and duplication syndromes: a clinical spectrum varying from non-pathogenic to a severe outcome. J. Med. Genet. *46*, 511–523.

3. Liao, J., DeWard, S.J., Madan-Khetarpal, S., Surti, U., and Hu, J. (2011). A small homozygous microdeletion of 15q13.3 including the CHRNA7 gene in a girl with a spectrum of severe neurodevelopmental features. Am. J. Med. Genet. A. *155A*, 2795–2800.

4. Lepichon, J.-B., Bittel, D.C., Graf, W.D., and Yu, S. (2010). A 15q13.3 homozygous microdeletion associated with a severe neurodevelopmental disorder suggests putative functions of the TRPM1, CHRNA7, and other homozygously deleted genes. Am. J. Med. Genet. A. *152A*, 1300–1304.

5. Shinawi, M., Schaaf, C.P., Bhatt, S.S., Xia, Z., Patel, A., Cheung, S.W., Lanpher, B., Nagl, S., Herding, H.S., Nevinny-Stickel, C., et al. (2009). A small recurrent deletion within 15q13.3 is associated with a range of neurodevelopmental phenotypes. Nat. Genet. *41*, 1269–1271.

6. Lowther, C., Costain, G., Stavropoulos, D.J., Melvin, R., Silversides, C.K., Andrade, D.M., So, J., Faghfoury, H., Lionel, A.C., Marshall, C.R., et al. (2015). Delineating the 15q13.3 microdeletion phenotype: a case series and comprehensive review of the literature. Genet. Med. *17*, 149–157.

7. Gillentine, M.A., and Schaaf, C.P. (2015). The human clinical phenotypes of altered CHRNA7 copy number. Biochem. Pharmacol. *97*, 352–362.

8. Hoppman-Chaney, N., Wain, K., Seger, P.R., Superneau, D.W., and Hodge, J.C. (2013). Identification of single gene deletions at 15q13.3: further evidence that CHRNA7 causes the 15q13.3 microdeletion syndrome phenotype. Clin. Genet. *83*, 345–351.

9. Yin, J., Chen, W., Yang, H., Xue, M., and Schaaf, C.P. (2017). Chrna7 deficient mice manifest no consistent neuropsychiatric and behavioral phenotypes. Sci. Rep. *7*, 39941.

10. Fotaki, V., Dierssen, M., Alcántara, S., Martínez, S., Martí, E., Casas, C., Visa, J., Soriano, E., Estivill, X., and Arbonés, M.L. (2002). Dyrk1A haploinsufficiency affects viability and causes developmental delay and abnormal brain morphology in mice. Mol. Cell. Biol. *22*, 6636–6647.

12. Hao, S., Tang, B., Wu, Z., Ure, K., Sun, Y., Tao, H., Gao, Y., Patel, A.J., Curry, D.J., Samaco, R.C., et al. (2015). Forniceal deep brain stimulation rescues hippocampal memory in Rett syndrome mice. Nature *526*, 430–434.

13. Parnass, Z., Tashiro, A., and Yuste, R. (2000). Analysis of spine morphological plasticity in developing hippocampal pyramidal neurons. Hippocampus *10*, 561–568.

14. Spielmann, M., Reichelt, G., Hertzberg, C., Trimborn, M., Mundlos, S., Horn, D., and Klopocki, E. (2011). Homozygous deletion of chromosome 15q13.3 including CHRNA7 causes severe mental retardation, seizures, muscular hypotonia, and the loss of KLF13 and TRPM1 potentially cause macrocytosis and congenital retinal dysfunction in siblings. Eur. J. Med. Genet. *54*, e441–e445.

15. Endris, V., Hackmann, K., Neuhann, T.M., Grasshoff, U., Bonin, M., Haug, U., Hahn, G., Schallner, J.C., Schröck, E., Tinschert, S., et al. (2010). Homozygous loss of CHRNA7 on chromosome 15q13.3 causes severe encephalopathy with seizures and hypotonia. Am. J. Med. Genet. A. *152A*, 2908–2911.

16. Masurel-Paulet, A., Andrieux, J., Callier, P., Cuisset, J.M., Le Caignec, C., Holder, M., Thauvin-Robinet, C., Doray, B., Flori, E., Alex-Cordier, M.P., et al. (2010). Delineation of 15q13.3 microdeletions. Clin. Genet. *78*, 149–161.

17. Shu, W., Cho, J.Y., Jiang, Y., Zhang, M., Weisz, D., Elder, G.A., Schmeidler, J., De Gasperi, R., Sosa, M.A.G., Rabidou, D., et al. (2005). Altered ultrasonic vocalization in mice with a disruption in the Foxp2 gene. Proc. Natl. Acad. Sci. USA *102*, 9643–9648.

18. Scattoni, M.L., Crawley, J., and Ricceri, L. (2009). Ultrasonic vocalizations: a tool for behavioural phenotyping of mouse models of neurodevelopmental disorders. Neurosci. Biobehav. Rev. *33*, 508–515.

19. Peñagarikano, O., Abrahams, B.S., Herman, E.I., Winden, K.D., Gdalyahu, A., Dong, H., Sonnenblick, L.I., Gruver, R., Almajano, J., Bragin, A., et al. (2011). Absence of CNTNAP2 leads to epilepsy, neuronal migration abnormalities, and core autism-related deficits. Cell *147*, 235–246.

20. Forsingdal, A., Fejgin, K., Nielsen, V., Werge, T., and Nielsen, J. (2016). 15q13.3 homozygous knockout mouse model display epilepsy-, autism- and schizophrenia-related phenotypes. Transl. Psychiatry *6*, e860.

21. Zhang, Y., Chen, K., Sloan, S.A., Bennett, M.L., Scholze, A.R., O'Keeffe, S., Phatnani, H.P., Guarnieri, P., Caneda, C., Ruderisch, N., et al. (2014). An RNA-sequencing transcriptome and splicing database of glia, neurons, and vascular cells of the cerebral cortex. J. Neurosci. *34*, 11929–11947.

22. Urbé, S., Liu, H., Hayes, S.D., Heride, C., Rigden, D.J., and Clague, M.J. (2012). Systematic survey of deubiquitinase localization identifies USP21 as a regulator of centrosome- and microtubule-associated functions. Mol. Biol. Cell *23*, 1095–1103.

23. Uddin, M., Unda, B.K., Kwan, V., Holzapfel, N.T., White, S.H., Chalil, L., Woodbury-Smith, M., Ho, K.S., Harward, E., Murtaza, N., et al. (2018). OTUD7A regulates neurodevelopmental phenotypes in the 15q13.3 microdeletion syndrome. Am. J. Hum. Genet. *102*, this issue, 278–295.

24. Drapeau, E., Dorr, N.P., Elder, G.A., and Buxbaum, J.D. (2014). Absence of strong strain effects in behavioral analyses of Shank3-deficient mice. Dis. Model. Mech. *7*, 667–681.

25. Bi, W., Ohyama, T., Nakamura, H., Yan, J., Visvanathan, J., Justice, M.J., and Lupski, J.R. (2005). Inactivation of Rai1 in mice recapitulates phenotypes observed in chromosome engineered mouse models for Smith-Magenis syndrome. Hum. Mol. Genet. *14*, 983–995.

26. Guy, J., Hendrich, B., Holmes, M., Martin, J.E., and Bird, A. (2001). A mouse Mecp2-null mutation causes neurological symptoms that mimic Rett syndrome. Nat. Genet. *27*, 322–326.

27. Mikhail, F.M., Lose, E.J., Robin, N.H., Descartes, M.D., Rutledge, K.D., Rutledge, S.L., Korf, B.R., and Carroll, A.J. (2011). Clinically relevant single gene or intragenic deletions encompassing critical neurodevelopmental genes in patients with developmental delay, mental retardation, and/or autism spectrum disorders. Am. J. Med. Genet. A. *155A*, 2386–2396.

28. Prasun, P., Hankerd, M., Kristofice, M., Scussel, L., Sivaswamy, L., and Ebrahim, S. (2014). Compound heterozygous microdeletion of chromosome 15q13.3 region in a child with hypotonia, impaired vision, and global developmental delay. Am. J. Med. Genet. A. *164A*, 1815–1820.

Supplemental Data

Otud7a Knockout Mice Recapitulate

Many Neurological Features

of 15q13.3 Microdeletion Syndrome

Jiani Yin, Wu Chen, Eugene S. Chao, Sirena Soriano, Li Wang, Wei Wang, Steven E. Cummock, Huifang Tao, Kaifang Pang, Zhandong Liu, Fred A. Pereira, Rodney C. Samaco, Huda Y. Zoghbi, Mingshan Xue, and Christian P. Schaaf

Material and Methods for Supplementary Figures

Elevated plus maze

Anxiety was assessed, using the elevated plus maze, as described previously [1]. Mice at 10 weeks of age were put at the cross area of the maze in white, facing the open arm. The maze was elevated 50 cm from the floor. Activity data was collected over a 10 min period, using the Fusion software (Omnitech electronics) version 4.75.

Open field activity

Locomotor activity and anxiety level were assessed at 10 weeks of age, using the open field assay, as described previously [1]. Activity in a clear acrylic (40 cm × 40 cm × 30 cm) open field arena was recorded over a 30 min period, using the Fusion software version 3.7.

Light-dark box exploration

Anxiety was also assessed in the light-dark box at 10 weeks of age. The apparatus is composed of two adjoining chambers made of plexiglas: a small enclosed chamber (15 cm × 21 cm × 21 cm) with black walls, and a larger chamber (30 cm × 21 cm × 21 cm) with transparent walls and an open top. The two chambers were connected by a small opening. Mice were placed into the illuminated (750 lux) larger chamber and allowed to explore freely for 10 min. Activity data, including the number and latency of entries, and time spent in each compartment, was collected using the Fusion software version 3.7.

Self-grooming

The self-grooming test was used to evaluate compulsive grooming behaviors, as described previously [1]. Each mouse was placed individually into a standard mouse cage with a thin layer of bedding, habituated for at least 30 min, and was then videotaped for

10 min. Time spent on spontaneous grooming of any part of its face, body, limbs, or tail was quantified and subsequently analyzed.

Holeboard exploration

The holeboard exploration test was used to evaluate repetitive nose-poke behavior. Mice at 10 weeks of age were placed into a clear acrylic (40 cm × 40 cm × 30 cm) chamber with a black 16-hole floorboard. Holeboard exploration data was collected, using the Fusion software version 7.7. The number of total and sequential nose-pokes in a 10 min period was quantified.

Forced swimming test

Depression-related behavior was assessed, using the forced swimming test, as previously described [1]. Mice at 12 weeks of age were placed into a 22 cm diameter circular tank with 17 cm deep water at room temperature for 6 min. Immobility time was defined as the duration in which the percentage of immobility was greater than 88% during any 500 msec period. This was automatically determined using the ANY-Maze Video Tracking System version 4.75 (Stoelting Co., IL).

Three-chamber test

Sociability was assessed at 12 weeks of age, using the three-chamber test, as described previously [1]. After a 10 min habituation period, a sex- and age-matched C57BL/6J mouse was placed under one wire cup, and a lego object of similar size and color was placed under the wire cup in the opposite compartment. Test mice were then allowed to explore freely for another 10 min. Data of time spent in each compartment, and the amount of time spent in close contact with each wire cup in the two phases were determined, using

ANY-Maze version 4.75 and manual scoring. Due to seizure occurrence during the test period, one male null mouse was excluded from data analysis of three-chamber test.

Partition test

Interest in social novelty was assessed using the partition test, as described previously [1]. At 12 weeks of age, each test mouse was housed overnight with an age- and sex-matched C57BL/6J partner mouse in the two separate compartments of a partition cage. The next day, activity at the partition board was measured, first with the familiar overnight partner, followed by an unfamiliar partner, and then back to the original familiar partner, for 5 min each. This was manually scored using a Psion Handheld Computer and Observer XT (Noldus Information Technology, Netherlands).

Conditioned fear

Conditioned fear was used to evaluate learning and memory at 13 weeks of age. On the training day, mice were placed into the isolation cubicles (Coulbourn Instruments, PA) and allowed to explore for 2 min. The conditioned stimulus (CS, a white noise 80 dB sound) was then presented for 30 sec and was followed immediately by a mild foot shock (2 sec, 0.7 mA) that served as the unconditioned stimulus (US). The conditioning pattern (2 min rest followed by 30 sec sound stimulus that was paired with foot shock) was then repeated once. Mice were then returned to their homecages. Timing of CS and US presentations and percentage freezing were monitored and assessed using the freezeframe software (Coulbourn instruments, PA).

Approximately 24h after training, mice were placed back into the original chamber to test for contextual fear conditioning. Freezing was recorded over a 5 min period. One hour later, mice were placed into a new chamber with different contextual cues to test for

auditory cued conditioned fear. White Plexiglas inserts were placed on both the floor and sides of the chamber to alter the shape, texture, and color of the chamber, and vanilla extract was placed in the chamber behind the insert to alter the odor. In addition, light condition in the testing room was changed to dim red light. Mice were brought into the room in transfer cages that contained paper towels instead of bedding, and then placed into the new chamber. Freezing was recorded for 3 min during a "pre-CS" phase, followed by another 3 min while the auditory CS was presented.

Nest building

Nest building was evaluated at 14 weeks of age to test for home cage social behaviors, as described previously [2]. Mice were single-housed after the conditioned fear test and a nestlet (5 cm squares of cotton batting) was placed into the cage around 6:00 PM. The following day between 10-11 AM, nest quality was scored on a 5-point scale by an experimenter who was blind to the genotypes, based on the shape and height of the nests [2].

Novel object recognition

Novel object recognition was used to evaluate the memory of mice at 27 weeks of age. The habituation chamber and test chamber were both transparent plastic chambers (40cm x 24 cm x 20 cm) with no top. The test chamber was surrounded by white boards on three sides (all but the side that faced the observer), with white paper on the bottom. At the side farthest from the observer, three mirrors were placed to assist observation and scoring. Two identical Lego objects for training were placed in the test chamber symmetrically, 5 cm away from the center. Mice were first habituated in the empty chamber for 5 min, and then transferred to the test chamber, in which they were allowed to explore for 5 min. The

test chamber was cleaned with 30% isopropanol between each mouse, to dissipate the odors. Mice were trained for three days. On the fourth day, we tested the mice by replacing one of the objects in the test chamber with a novel Lego object. As a control, on the fifth day, mice were presented the same objects from the training sessions. On all days, the time that mice interacted with each object was manually recorded.

Auditory Testing

Auditory Brainstem Responses (ABRs) and Distortion Product of the Otoacoustic Emissions (DPOAEs) were measured as previously described [3; 4]. Briefly, 3 month-old mice, 4 WT (♂), 4 HET (♂), 9 KO (♂), 3 WT (♀), 4 HET (♀), and 6 KO (♀), were anesthetized using an intraperitoneal injection of ketamine (100 mg/kg) and xylazine (10 mg/kg). Normal body temperature was maintained throughout the procedure by placing the mice on a heating pad. Pure tone stimuli from 4 kHz to 48 kHz (ABRs) or 8 kHz to 32 kHz (DPOAEs) were generated using Tucker Davis Technologies System 3 digital signal processing hardware and software (Tucker Davis Technologies, Alachua, FL, USA), and the intensity of the tone stimuli was calibrated using a type 4938 1/4″ pressure-field calibration microphone (Brüel and Kjær, Nærum, Denmark). ABR signals were recorded with subcutaneous needle electrodes inserted at the vertex of the scalp, the postauricular region (reference) and the back leg (ground) and the DPOAE distortion-products were captured with a microphone and preamplifier (ER-10B+, Etymotic Research, Inc.). Auditory thresholds were determined by decreasing the sound intensity of each stimulus in 5 dB steps (90 dB to 10 dB for ABRs; 75 dB to 40 dB for DPOAEs) until the lowest sound intensity with reproducible and recognizable ABR waveforms or

2f1-f2 distortion-products was reached. Statistical analysis was performed using Three-way ANOVA with repeated measures.

HeLa cell culture and transfection

HeLa cells were ordered from American Type Culture Collection (ATCC) and cultured in DMEM (Thermo Fisher Scientific, Ca. 11330032) containing 10% FBS and 1% Penicillin/Streptomycin. The cells were tested to be mycoplasma free. Cells were around 90% confluent at the time of transfection. For cells in a 12-well plate, 75 μl Opti-MEM (Invitrogen, Ca. 31985-070) and 3μl Lipofectamine 2000 were mixed and incubated for 5 min. At the same time, 75 μl of Opti-MEM and 400 ng of each plasmid were mixed and incubated for 5 min. Then, the DNA mixture was added to the Lipofectamine mixture and incubated for 20 min, prior to adding them to the cells.

Sholl analysis

Image stacks were imported to the confocal module of Neurolucida 360 (MicroBrightfield, Inc., Williston, VT), and neuronal dendritic trees were traced in interactive mode. Sholl analysis was performed for each traced neuron by automatically calculating the number of dendritic intersections and the dendritic length at 10-μm interval starting from the soma. Soma area was determined by manually defined soma contours and automatic detection of area over a pre-set thickness threshold. Primary neuronal culture and Sholl analysis have been repeated three times. In total, we investigated 27 primary neurons from wild-type and 26 primary neurons from homozygous knockout mice on DIV 14. Data were analyzed blindly to the genotypes. Statistical analysis was performed using Two-way ANOVA with Tukey's multiple comparisons test.

References

1. Yin, J., Wu, C., Yang, H., Xue, M., and Schaaf, Christian P. (2017). Chrna7 deficient mice manifest no consistent neuropsychiatric and behavioral phenotypes. Scientific reports 7.
2. Deacon, R.M.J. (2006). Assessing nest building in mice. Nat Protocols 1, 1117-1119.
3. Xia, A., Song, Y., Wang, R., Gao, S.S., Clifton, W., Raphael, P., Chao, S.-i., Pereira, F.A., Groves, A.K., and Oghalai, J.S. (2013). Prestin regulation and function in residual outer hair cells after noise-induced hearing loss. PloS one 8, e82602.
4. Cai, T., Seymour, M.L., Zhang, H., Pereira, F.A., and Groves, A.K. (2013). Conditional deletion of Atoh1 reveals distinct critical periods for survival and function of hair cells in the organ of Corti. Journal of Neuroscience 33, 10110-10122.

Figure S1
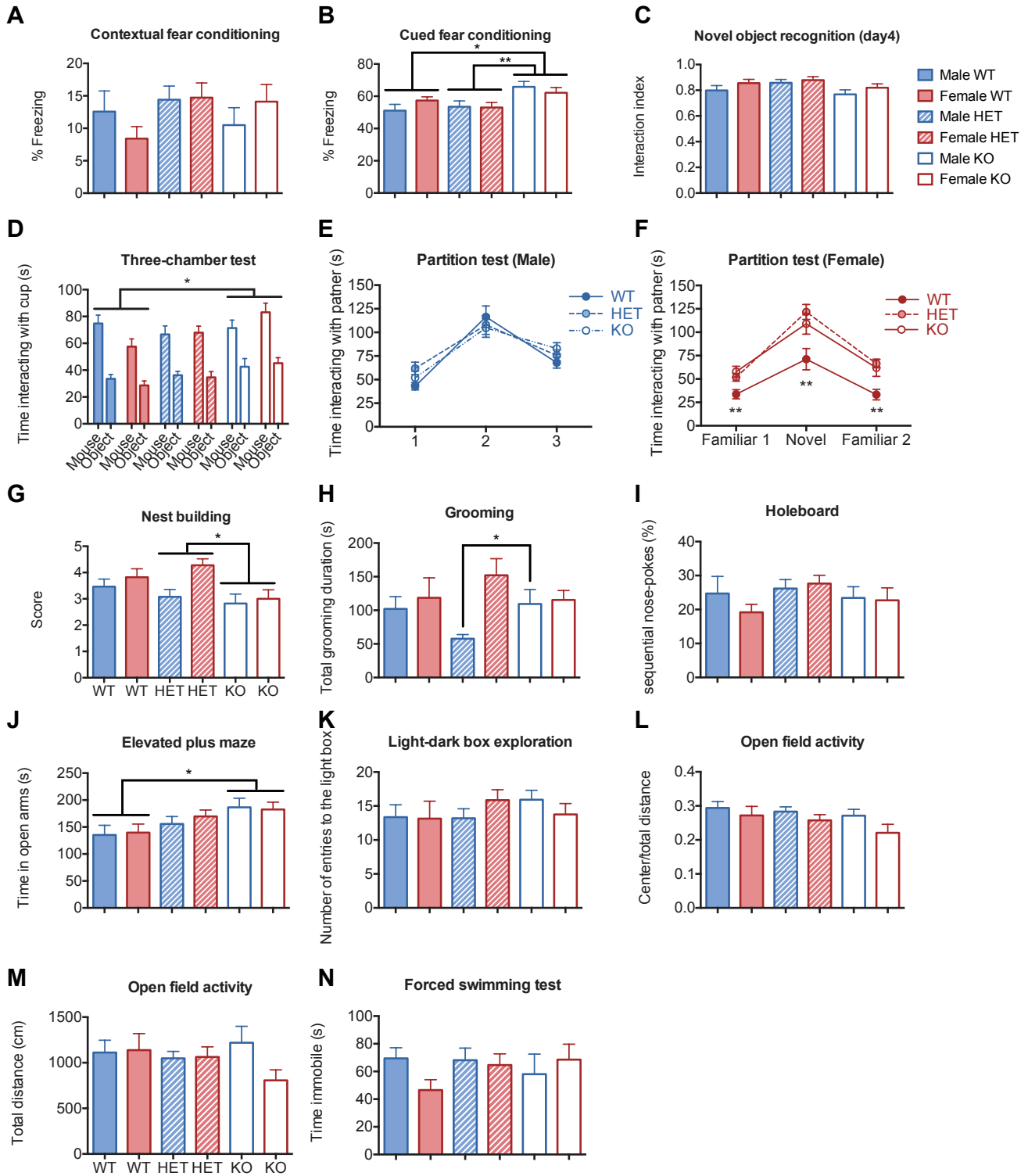
Figure S1 Additional behavioral phenotypes of mice deficient in *Otud7a*. Behavioral data from male and female adult mice were shown separately, with males in blue and females in red. **A-B**, Null mice show no impairment in learning and memory in contextual or cued fear conditioning. **C**, Null mice show no significant impairment in novel object recognition. **D**, Null mice do not show reduced sociability in three-chamber test. **E-F**, Neither male or female null mice show reduced social novelty in partition test. **G**, Null mice do not show impairment in nest building compared to wild-type littermates. **H**, Null mice do not show repetitive behavior in self-grooming. **I**, Null mice do not show repetitive behavior in holeboard exploration. **J**, Null mice do not show significant difference in anxiety-like behavior, measured by time in the open arms in elevated plus maze. **K**, Null mice do not show anxiety-like behavior in light-dark box test, measured by number of entries into the light box. **L**, Null mice do not show anxiety-like behavior in open field activity, measured by center/total distance. **M**, Null mice do not show significant difference in open field activity, measured by total distance run. **N**, Null mice do not display depression-like behavior in forced swimming test, measured by percent time immobile. Each point represents the mean ± SEM (*$P < 0.05$, ** $P < 0.01$).

Figure S2

Auditory brain stem responses (male)

Auditory brain stem responses (female)

DPOAE (male)

DPOAE (female)
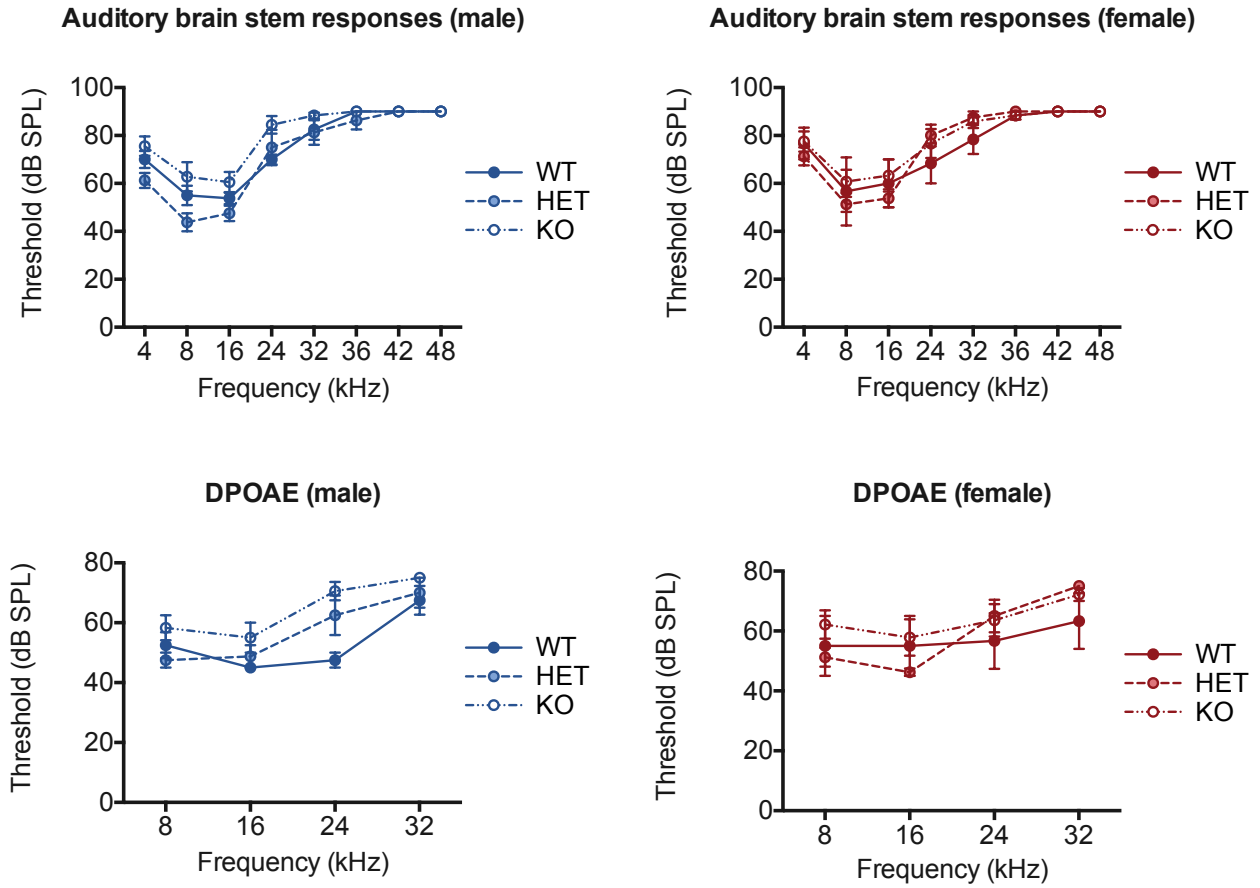
Figure S2 Hearing ability of *Otud7a* knockout mice is not different from wild-type littermates. Auditory Brainstem Response (ABR) and Distortion Product of Otoacoustic Emissions (DPOAEs) were determined for wild-type and *Otud7a* knockout mice to assess hearing at 3 month-old. Data are presented as mean ± SEM.

Figure S3

	anti-FLAG	Merge
3xFLAG-OTUD7A		
HA-FLAG-EGFP		
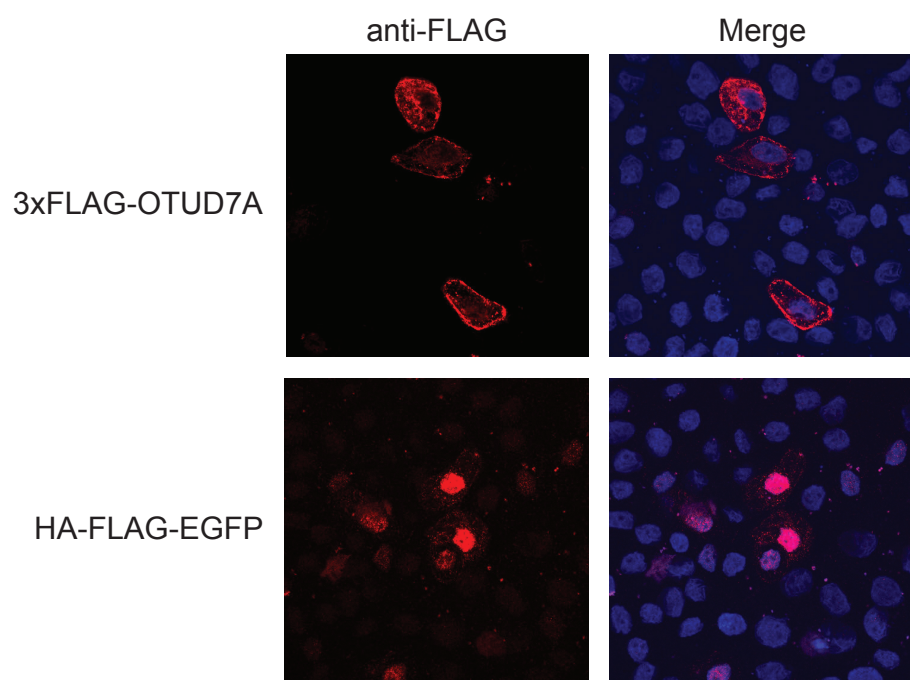
Figure S3 OTUD7A localizes to the membrane compartments in HeLa cells. HeLa cells were ordered from American Type Culture Collection (ATCC) and cultured in DMEM (Thermo Fisher Scientific, Ca. 11330032) containing 10% FBS and 1% Penicillin/Streptomycin. The cells were tested to be mycoplasma free. Cells were around 90% confluent at the time of transfection. For cells in a 12-well plate, 75 µl Opti-MEM (Invitrogen, Ca. 31985-070) and 3µl Lipofectamine 2000 were mixed and incubated for 5 min. At the same time, 75 µl of Opti-MEM and 400 ng of each plasmid were mixed and incubated for 5 min. Then, the DNA mixture was added to the Lipofectamine mixture and incubated for 20 min, prior to adding them to the cells. 3xFLAG-OTUD7A was detected on plasma membrane and other membrane compartments after overexpression in HeLa cells. In the control, HA-FLAG-EGFP localizes to the nucleus and cytoplasm after overexpression in HeLa cells. Over-expressed proteins were stained with FLAG antibody (red), and the nucleus was stained with DAPI (blue).
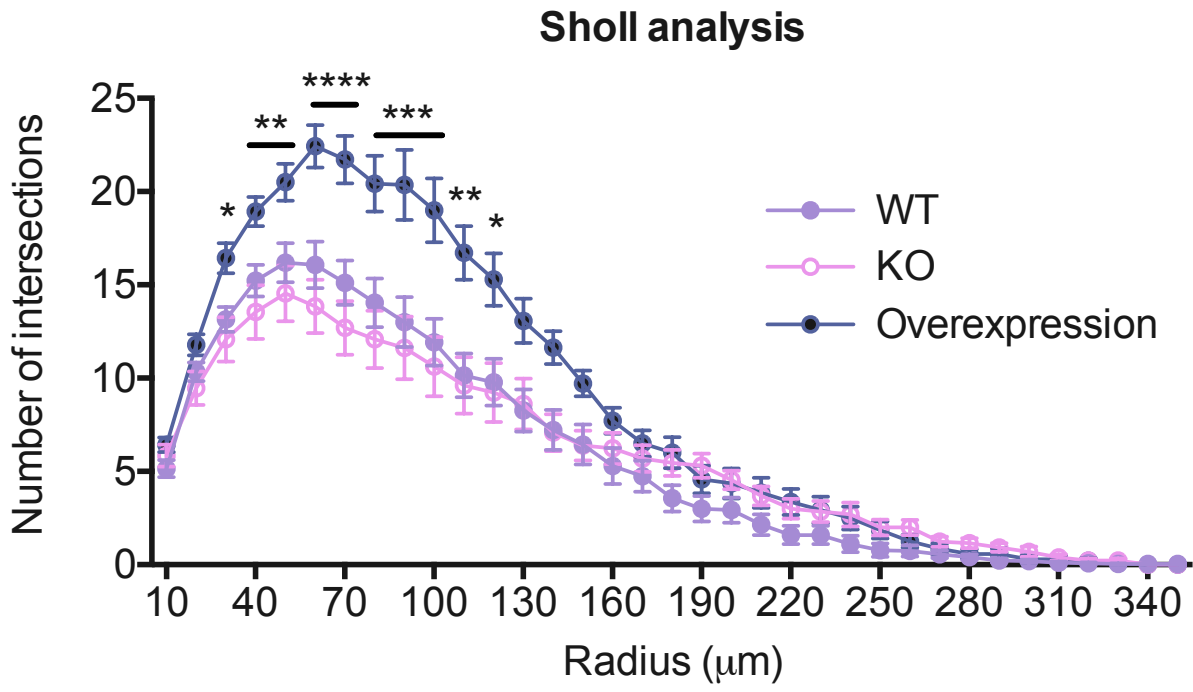
Sholl analysis

Figure S4 Sholl analysis of primary neurons indicates a potential role of Otud7a in dendritic complexity. Image stacks were imported to the confocal module of Neurolucida 360 (MicroBrightfield, Inc., Williston, VT), and neuronal dendritic trees were traced in interactive mode. Sholl analysis was performed for each traced neuron by automatically calculating the number of dendritic intersections and the dendritic length at 10-μm interval starting from the soma. Soma area was determined by manually defined soma contours and automatic detection of area over a pre-set thickness threshold. Primary neuronal culture and Sholl analysis have been repeated three times. In total, we investigated 27 primary neurons from wild-type and 26 primary neurons from homozygous knockout mice on DIV 14. Data were analyzed blindly to the genotypes. Statistical analysis was performed using Two-way ANOVA with Tukey's multiple comparisons test. Primary neurons (n= 26-27) from *Otud7a* null mice showed no significant difference from wild-type, however, overexpression of *Otud7a* (n =18) led to significantly increased dendritic complexity. Data were obtained from 6 *Otud7a* null mice and 3 wild-type littermates. Data are presented as mean ± SEM (*$P < 0.05$, ** $P < 0.01$, *** $P < 0.001$, **** $P < 0.0001$).

Table S1. sgRNA off-target candidates and primers used to amplify the corresponding regions.

sgRNA	off-target candidates	Forward primer	Reverse primer
CTAGCGAGGCGGCATGTAAG	AGAGTGCTTCCTTAGCAAGGCGG	AAGGCAGGAACTCTGCATTG	TCCCGTCTGATCATCCTTTC
	AGACTGCCTACCTAGGGAGGGAG	TGGGTGACTCTTGTCTGTGG	AGTCTGCGGTGAAATGGAAT
	AGAGTGCTTCCCTAGCAAGCCAG	AGTGGGCCTCTTTCTGGAAT	AAGTCATAGCCCAGCAGTGG
	AAAGTGCTTACCCAGCCAGGGAG	GGCAATAGGAACCAGTCCAA	ACAAGCCATTTCTTGGCATC
	AGGGTTCTTCCCTAGAGAGGGAG	GGGATTGATGTTTTGGTGCT	ACACCCAGCTGGAAGCTCTA
	TGGGTCCCTACCTAGCCAGGAAG	TTTCATCATGACCCCTGACA	TTCATTTTGCACAGCTCAGG
	AAGGTCCTTCCTTAGCGAGGCAG	CCAGGTCTTGCACACAGCTA	TGGGGATCAAACTCAAGGTC
	AGGGAGCTTCCCTAGGGAGGAAG	CCCAGTCCTGCTTTAACCAA	ACTTGCCCAAAGTCACCATC
	AGGGTGCCTGACTAGCAAGGCAG	TGACTAGCAAGGCAGCTTGA	ACTCCACACTCTGGCTGAGG
	TGGTTGCTTCCCTAGGGAGGAGG	CATCAGGCAAAACTGACCAA	TAGATGGCCTTGTTGGCTTC
	AGGGTCATTGCCTAGCGAGCTGG	CCTCATTGGCACTTCCTGAT	GTGGGACCTCTTCTGCTCTG
	AAGGTGCTTATCTAGAGAGGCAG	AACCAGGTGTCTGCAAATGA	GCAATGTGGAAGCACCTTTT
	AGGGTGCGTACATAGCGTGGCAG	ATGCTTCTCCAAGGGAGGAT	ATGTGGGCTGCGATCTTATC
	AGGAAGCTTCCCTAGGGAGGGAG	AGTGGGAAACACAGCTCCAG	TCACTTCACCTGACCAGCAC
	ATGGTGATTTCCTAGCTAGGGAG	AAGGGTGGCTTCAGACTTGA	TGACAAGTAGAGGCAGGAGGA
GAAGTGTGTGCGAGGCTCGC	GAAGGGGGAGGGAGGCTCGCTGG	GAGGTGGGATCTTCTGGACA	TGTGGCAGAAGGTGAGTGAG
	GCAGTGCACGCGAGGCTCGCGGG	TGCTAGCGGTTTCCTGACTT	ACAGTGAGGGAGAGCGATGT
	GAGGTGTGTGGGAGGCTGGCTAG	GAGCCACCTTAACCACCGTA	ATTCCACTTTGGTTGCCAAG
	GACGCCTGTGCGGGGCTCGCCGG	GCCATCCTGTCGGTGAAC	ACGCCTCAGTTTTTCCACAC
	GAAGTGTCTGAGAGGCTGGCTGG	ATCTGCCACCCTCACTAAGC	CTGGGCTGACTCAGAAGAGC
	GGAGTGGCTGAGAGGCTCGCTGG	AACCTGTCCCTCATTTGTGC	CACTGCAAACCTGGGAATTT
	TAAGTGTCTGCGATGCTCGCTGG	CAAAACAAGCGTCCTCCATT	AGGAAAAGCTGAGCCAATGA
	GGAATGTGTGCGAGGCTCACAGG	GTGAGGCAGAAGGGTCATGT	AGTGTCTGCATCAGCAGTGG
	GGAGGCTGTGAGAGGCTCGCAAG	CACCAATCCAATTGTGTCGT	GCTTGGTTAGCCTGCTCATT
	GTGGTGTATGCCAGGCTCGCCAG	GGAGGTGACTCCATGGCTAA	TTGCTCACACATTTGCTTCC
	GTGGTGTATGCCAGGCTCGCCAG	GGAGGTGACTCCATGGCTAA	TTGCTCACACATTTGCTTCC
	GTGGTGTATGCCAGGCTCGCCAG	GGAGGTGACTCCATGGCTAA	TTGCTCACACATTTGCTTCC
	GTGGTGTATGCCAGGCTCGCCAG	GGAGGTGACTCCATGGCTAA	TTGCTCACACATTTGCTTCC
	GAAGGGTAGGCGAGGCCCGCTGG	AATGAGCACCGGGAAGTAAA	ACTCGGAGGCTGTGGTTATG
	GAAGTGTCTGTGAGGCGCGCGAG	CCAAGCGTCCTTTACCTCAG	GGCACCTCGAATCTTTGCTA

Table S2. Lipid modification sites predicted in human and mouse OTUD7A and OTUD7B proteins by GPS-lipid software.

ID	Position	Peptide	Type	Score
hOTUD7A	14	PNPTSAE<u>C</u>WAALLHD	S-Palmitoylation	6.60
	137	RSHVASE<u>C</u>NNEQFPL	S-Palmitoylation	2.33
	196	WSTVCTS<u>C</u>KRLLPLA	S-Palmitoylation	1.26
	794	AVGALRP<u>C</u>ATYPQQN	S-Palmitoylation	1.96
hOTUD7B	-	-	-	-
mOTUD7A	14	PNPPSAE<u>C</u>WAALLHD	S-Palmitoylation	7.23
	102	GHKVERP<u>C</u>LQRQDDI	S-Palmitoylation	2.81
	198	WSTVCTS<u>C</u>KRLLPLA	S-Palmitoylation	1.26
	802	TVGALRP<u>C</u>ATYPQQN	S-Palmitoylation	4.43
mOTUD7B	-	-	-	-

Table S3. Statistic analysis of behaviors in *Otud7a* mutant mice

Behavioral assay	Measurement	Statistical test	Comparison	Statistics	Defrees of freedom	P value	Post hoc		Adjusted P value	Interpretation	Fig.
Developmental delay	The first day of negative geotaxis	Kruskal-Wallis Test	Factor: Genotype	14.560	2	<0.001	Dunn's multiple comparison test	WT vs. HET	>0.999	KO has significant developmental delay in negative geotaxis.	Fig. 2b
								WT vs. KO	<0.001		
								HET vs. KO	0.003		
	The first day of cliff aversion	Kruskal-Wallis Test	Factor: Genotype	14.760	2	<0.001	Dunn's multiple comparison test	WT vs. HET	>0.999	KO has significant developmental delay in cliff aversion.	
								WT vs. KO	<0.001		
								HET vs. KO	0.005		
	The first day of incisor eruption	Kruskal-Wallis Test	Factor: Genotype	7.794	2	0.020	Dunn's multiple comparison test	WT vs. HET	>0.999	KO has significant developmental delay in incisor eruption.	
								WT vs. KO	0.029		
								HET vs. KO	0.046		
	The first day of incisor growth	Kruskal-Wallis Test	Factor: Genotype	7.041	2	0.030	Dunn's multiple comparison test	WT vs. HET	0.205	KO has significant developmental delay in incisor growth.	
								WT vs. KO	0.030		
								HET vs. KO	0.913		
	The first day of eye lid opening	Kruskal-Wallis Test	Factor: Genotype	5.188	2	0.075				KO is not significantly delayed in eye lid opening.	
	The first day of ear opening	Kruskal-Wallis Test	Factor: Genotype	3.399	2	0.183				KO is not significantly delayed in ear opening.	
Ultrasonic vocalization	Number of vocalizations	Two-Way ANOVA with repeated measures	Factor1: Genotype	8.946	2, 61	<0.001	Tukey's multiple comparison test	PND2 WT vs. HET	0.954		Fig. 2c
								PND2 WT vs. KO	0.357	KO is not significantly different in vocalizaiton on postnatal day 2.	
								PND2 HET vs. KO	0.414		
								PND4 WT vs. HET	0.843		
								PND4 WT vs. KO	0.345	KO is not significantly different in vocalizaiton on postnatal day 4.	
								PND4 HET vs. KO	0.568		
								PND6 WT vs. HET	0.198		
								PND6 WT vs. KO	0.018	KO has significantly reduced vocalizations on postnatal day 6.	
								PND6 HET vs. KO	0.381		
								PND8 WT vs. HET	0.463		
								PND8 WT vs. KO	0.030	KO has significantly reduced vocalizations on postnatal day 8.	
								PND8 HET vs. KO	0.214		
								PND10 WT vs. HET	0.011	HET has significantly reduced vocalizations on postnatal day 10.	
								PND10 WT vs. KO	0.012	KO has significantly reduced vocalizations on postnatal day 10.	
								PND10 HET vs. KO	0.972		
			Factor2 (repeated): Day	3.647	4, 244	0.007					
			Interaction (F1 x F2)	0.702	8, 244	0.690					
Conditioned fear	Freezing in contextual fear conditioning (%)	Two-Way ANOVA	Factor1: Genotype	1.403	2, 93	0.251				KO is not significantly different in contextual fear conditioning.	Sup Fig. 1a
			Factor2: Sex	0.001	1, 93	0.971					
			Interaction (F1 x F2)	1.110	2, 93	0.334					
	Freezing in cued fear conditioning (%)	Two-Way ANOVA	Factor1: Genotype	6.160	2, 93	0.003	Tukey's multiple comparison test	WT vs. HET	0.953		Sup Fig. 1b
								WT vs. KO	0.022	KO has significantly increased cued fear conditioning.	
								HET vs. KO	0.005		
			Factor2: Sex	0.068	1, 93	0.795					
			Interaction (F1 x F2)	1.025	2, 93	0.363					
Novel object recognition	Interaction index (Ratio of time interacting with novel/familiar object)	Two-Way ANOVA	Factor1: Genotype	3.050	2, 95	0.052					Sup Fig. 1c
			Factor2: Sex	2.948	1, 95	0.089					
			Interaction (F1 x F2)	0.207	2, 95	0.814					
Rotarod	Latency to fall (s)	Three-Way ANOVA with repeated measures	Factor1: Genotype	20.857	2, 80	<0.001	Tukey's multiple comparison test	WT vs. HET	>0.999		Fig. 2e-f
								WT vs. KO	<0.001	KO has significantly reduced motor coordination.	
								HET vs. KO	<0.001		
			Factor2: Sex	0.664	1, 80	0.418					
			Factor3 (repeated): Trial	19.649	7, 560	<0.001					
			Interaction (F1 x F2)	2.315	2, 80	0.105					
			Interaction (F1 x F3)	2.068	14, 560	0.012	Tukey's multiple comparison test	WT vs. HET	0.980		

Test	Measure	Statistical test	Factor	F	df	p	Post-hoc test	Comparison	p	Note	Figure
								WT vs. KO	<0.001	KO has significantly reduced motor learning	
								HET vs. KO	<0.001		
			Interaction (F2 x F3)	0.755	7, 560	0.626					
			Interaction (F1x F2 x F3)	2.417	14, 560	0.003					
Acoustic startle	Response amplitude	Two-Way ANOVA	Factor1: Genotype	35.970	2, 92	<0.001	Tukey's multiple comparison test	WT vs. HET	0.002		Fig. 2g
								WT vs. KO	<0.001	KO has significant acoustic startle deficit.	
								HET vs. KO	<0.001		
			Factor2: Sex	4.910	1, 92	0.029					
			Interaction (F1 x F2)	1.678	2, 92	0.192					
Prepulse inhibition	Prepulse inhibition at 74 dB prepulse intensity (%)	Two-Way ANOVA	Factor1: Genotype	2.071	2, 98	0.132				KO is not significantly different in prepulse inhibition at 74 db prepulse intensity.	Fig. 2h-i
			Factor2: Sex	2.125	1, 98	0.148					
			Interaction (F1 x F2)	0.887	2, 98	0.415					
	Prepulse inhibition at 78 dB prepulse intensity (%)	Two-Way ANOVA	Factor1: Genotype	1.397	2, 98	0.252				KO is not significantly different in prepulse inhibition at 78 db prepulse intensity.	
			Factor2: Sex	1.863	1, 98	0.176					
			Interaction (F1 x F2)	2.354	2, 98	0.101					
	Prepulse inhibition at 82 dB prepulse intensity (%)	Two-Way ANOVA	Factor1: Genotype	7.916	2, 98	0.001					
			Factor2: Sex	8.362	1, 98	0.005					
			Interaction (F1 x F2)	4.060	2, 98	0.020	Split data by sex				
		One-Way ANOVA on males	Factor: Genotype	1.719	2, 47	0.191					
		One-Way ANOVA on females	Factor: Genotype	10.240	2, 50	<0.001	Tukey's multiple comparison test	WT vs. HET	0.860		
								WT vs. KO	0.001	Female KO has significant prepulse inhibition deficit at 82 db prepulse intensity.	
								HET vs. KO	0.001		
Three-chamber test	Time interacting with cups (s)	Three-Way ANOVA with repeated measures	Factor1: Genotype	4.236	2, 91	0.017	Tukey's multiple comparison test	WT vs. HET	>0.999		Sup Fig. 1d
								WT vs. KO	0.022	KO has significantly increased interaction with cups on both sides.	
								HET vs. KO	0.072		
			Factor2: Sex	0.158	1, 91	0.692					
			Factor3 (repeated): Side	169.108	1, 91	<0.001					
			Interaction (F1 x F2)	2.227	2, 91	0.114					
			Interaction (F1 x F3)	0.135	2, 91	0.874					
			Interaction (F2 x F3)	0.001	1, 91	0.978					
			Interaction (F1x F2 x F3)	1.396	2, 91	0.253					
Partition test	Time interacting with partition board (s)	Three-Way ANOVA with repeated measures	Factor1: Genotype	8.244	2, 89	0.001					Sup Fig. 1e-f
			Factor2: Sex	7.438	1, 89	0.008					
			Factor3 (repeated): Partner mouse	101.076	2, 178	<0.001					
			Interaction (F1 x F2)	4.270	2, 89	0.017	Split data by sex				
			Interaction (F1 x F3)	0.294	4, 178	0.881					
			Interaction (F2 x F3)	2.446	2, 178	0.090					
			Interaction (F1x F2 x F3)	2.725	4, 178	0.031	Split data by sex				
		Two-Way ANOVA with repeated measures on males	Factor1: Genotype	0.427	2, 43	0.655					
			Factor2 (repeated): Partner mouse	41.423	2, 86	<0.001					
			Interaction (F1 x F2)	1.267	4, 86	0.290				Male KO is not significantly different in interest in social novelty.	
		Two-Way ANOVA with repeated measures on females	Factor1: Genotype	10.322	2, 46	<0.001	Tukey's multiple comparison test	WT vs. HET	<0.001		
								WT vs. KO	0.002	Female KO has significantly increased interaction with partners in general.	
								HET vs. KO	0.876	Female HET has significantly increased interaction with partners in general.	
			Factor2 (repeated): Partner mouse	66.470	2, 92	<0.001					
			Interaction (F1 x F2)	1.806	4, 92	0.134				Female KO is not significantly different in interest in social novelty.	
Nest building	Scores of nest	Two-Way ANOVA	Factor1: Genotype	3.927	2, 92	0.023	Tukey's multiple comparison test	WT vs. HET	0.986		Sup Fig. 1g
								WT vs. KO	0.068		

Test	Measure	Analysis	Effect	F	df	p	Post-hoc	Comparison	p	Conclusion	Figure
								HET vs. KO	0.029	KO has significantly reduced nest building ability (compared to HET).	
			Factor2: Sex	5.256	1, 92	0.024					
			Interaction (F1 x F2)	1.714	2, 92	0.186					
Self-grooming	Total grooming duration (s)	Two-Way ANOVA	Factor1: Genotype	0.088	2, 90	0.916				KO is not significantly different in grooming duration.	Sup Fig. 1h
			Factor2: Sex	5.775	1, 90	0.018					
			Interaction (F1 x F2)	3.428	2, 90	0.037	Split data by sex				
		One-Way ANOVA on males	Factor: Genotype	3.850	2, 45	0.029	Tukey's multiple comparison test	WT vs. HET	0.093		
								WT vs. KO	0.943		
								HET vs. KO	0.043	Not sure	
		One-Way ANOVA on females	Factor: Genotype	0.874	2, 45	0.424				Female KO is not significantly different in grooming duration.	
Holeboard exploration	Sequential nose-pokes (%)	Two-Way ANOVA	Factor1: Genotype	1.393	2, 81	0.254				KO is not significantly different in holeboard exploration.	Sup Fig. 1i
			Factor2: Sex	0.344	1, 81	0.559					
			Interaction (F1 x F2)	0.588	2, 81	0.558					
Grip strength	Grip strength (g)	Two-Way ANOVA	Factor1: Genotype	3.596	2, 95	0.031	Tukey's multiple comparison test	WT vs. HET	0.322		Fig. 2d
								WT vs. KO	0.026	KO has significantly reduced grip strength.	
								HET vs. KO	0.404		
			Factor2: Sex	4.668	1, 95	0.033					
			Interaction (F1 x F2)	0.185	2, 95	0.831					
Elevated plus maze	Time in open arms (s)	Two-Way ANOVA	Factor1: Genotype	4.477	2, 92	0.014	Tukey's multiple comparison test	WT vs. HET	0.207		Sup Fig. 1j
								WT vs. KO	0.010	KO has significantly increased axiety level in elevated plus maze.	
								HET vs. KO	0.294		
			Factor2: Sex	0.157	1, 92	0.693					
			Interaction (F1 x F2)	0.197	2, 92	0.821					
Light-dark box exploration	Number of entries to the light box	Two-Way ANOVA	Factor1: Genotype	0.437	2, 93	0.647				KO is not significantly different in axiety level.	Sup Fig. 1k
			Factor2: Sex	0.004	1, 93	0.949					
			Interaction (F1 x F2)	1.080	2, 93	0.344					
Open field activity	Center/total distance ratio	Two-Way ANOVA	Factor1: Genotype	1.603	2, 93	0.207				KO is not significantly different in axiety level.	Sup Fig. 1l
			Factor2: Sex	3.965	1, 93	0.049					
			Interaction (F1 x F2)	0.282	2, 93	0.755					
	Total distance traveled (cm)	Two-Way ANOVA	Factor1: Genotype	0.333	2, 93	0.717				KO is not significantly different in total activity.	Sup Fig. 1m
			Factor2: Sex	1.338	1, 93	0.250					
			Interaction (F1 x F2)	1.785	2, 93	0.174					
Forced swimming test	Time immobile (%)	Two-Way ANOVA	Factor1: Genotype	0.369	2, 93	0.693				KO is not significantly different in depression-like behaviors.	Sup Fig. 1n
			Factor2: Sex	0.435	1, 93	0.511					
			Interaction (F1 x F2)	1.310	2, 93	0.275					
Hearing ABR test	Threshold (dB SPL)	Three-Way ANOVA with repeated measures	Factor1: Genotype	3.072	2, 25	0.064				KO is not significantly different in auditory brain stem responses.	Sup Fig. 2
			Factor2: Sex	0.338	1, 25	0.566					
			Factor3 (repeated): Frequency	11.817	5, 75	0.038					
			Interaction (F1 x F2)	0.236	2, 25	0.791					
			Interaction (F1 x F3)	2.554	2, 25	0.098					
			Interaction (F2 x F3)	0.677	1, 25	0.418					
			Interaction (F1x F2 x F3)	0.515	2, 25	0.604					
Hearing DPOAE test	Threshold (dB SPL)	Three-Way ANOVA with repeated measures	Factor1: Genotype	2.460	2, 24	0.107				KO is not significantly different in DPOAE.	Sup Fig. 2
			Factor2: Sex	0.446	1, 24	0.511					
			Factor3 (repeated): Frequency	99.622	7, 168	0.000					
			Interaction (F1 x F2)	0.666	2, 24	0.523					
			Interaction (F1 x F3)	2.231	14, 168	0.064					
			Interaction (F2 x F3)	0.922	7, 168	0.491					
			Interaction (F1x F2 x F3)	0.311	14, 168	0.992					